A DETERMINATION OF NEUTRON AND GAMMA DOSE RATES INSIDE THE D-RINGS AT WATERFORD-3 PRESSURIZED WATER REACTOR

A Thesis

Submitted to the Graduate Faculty of the
Louisiana State University and
Agricultural and Mechanical College
in partial fulfillment of the
requirements for the degree of
Master of Science

in

The Nuclear Science Center

by
Duane Foster McLane
B.E.T., Louisiana State University, 1987
August 1989

MANUSCRIPT THESES

Unpublished theses submitted for the Master's and Doctor's Degrees and deposited in the Louisiana State University Library are available for inspection. Use of any thesis is limited by the rights of the author. Bibliographical references may be noted, but passages may not be copied unless the author has given permission. Credit must be given in subsequent written or published work.

A library which borrows this thesis for use by its clientele is expected to make sure that the borrower is aware of the above restrictions.

LOUISIANA STATE UNIVERSITY LIBRARY

This Work is Dedicated To David Jerome McLane (1958-1988)

ACKNOWLEDGEMENTS

I wish to express my greatest appreciation to Mr. Greg Espenan whose guidance and knowlegde provided me with the drive and interest to complete this project. I know my career will be based on the professionalism he has shown me.

I also wish to express my sincere gratitude to Dr. J.C. Courtney for his guidence in this thesis project and throughout my graduate studies. I am also indebted to Dr. Max Scott, and the remainder of the staff in the department.

I would like to thank Louisiana Power and Light and Waterford 3 personnel for their consideration and hospitality during my many visits to the plant site.

Without the help of Yvonne Thomas for administrative and personal friendship, life as a graduate student would not have been as much fun. I also would like to thank Richard Teague for computer and technical insight at times when I needed it most. Thanks also goes out to all graduate students in the department present during my research.

I lastly would like to thank Missy and my family for the support when my problems were high and my patience low.

TABLE OF CONTENTS

LIST OF TABLES

LIST OF FIGURES

ABSTRACT

The D-rings at Waterford 3 Pressurized Water Reactor are the biological shields which are inside the containment building, that support and surround the reactor coolant system. Previous dosimetric studies have been conducted inside containment, but none of these studies were designed to quantify the dose rates inside the D-rings. Knowledge of the radiation environment inside the D-rings while the reactor is operating at full power is required prior to allowing personnel to enter these areas at power.

The dose rates are determined using techniques of neutron activation, computer calculations, Thermoluminecent Dosimetry (TLD), and information from previous studies. The Point Kernel computer code QAD-CG is used to calculate the gamma dose rates and TLDs for the neutron dose rates.

In order to assess the response of the TLDs an estimation of the neutron energy spectra inside the D-rings must be determined. These spectra are estimated by neutron activation, measured data from other reactors, and previous instrumental surveys. Thermoluminescent dosimeter calibration factors determined in locations outside the D-rings are used to estimate appropriate calibration for the irradiated TLDs.

The estimated dose rates inside the D-rings ranged from 0.950 rem/hr to 10.9 rem/hr. It is concluded that the dose rates are acceptable for short stay times provided the entry into the D-rings is made from above rather than from below.

Chapter One

INTRODUCTION AND BACKGROUND

1.1 Introduction

In order to accurately interpret monitoring instruments and personnel dosimetry inside nuclear reactor containment structures the characterization of the neutron and gamma radiation fields is necessary. At the Louisiana Power and Light Waterford 3 Steam Electric Station the neutron and gamma radiation field present inside containment have been extensively studied (So85, Cl87), but the radiation environment inside the biological shield at full power has never been quantified. Although some routine maintenance activities have been performed inside the containment building, no entries by maintenance personnel have been made into the biological shields during reactor operation due to the suspected high dose rates. This thesis will attempt to quantify the neutron and gamma dose rates within the biological shield at full power using various techniques - computer models, neutron activation analysis, personnel dosimeters, and prior measurements at Waterford 3 and other power reactors. Neutron dose equivalent rates will be determined from Thermoluminescent Dosimeters (TLD) and the gamma dose rates from the Point Kernel computer code QAD-CG and previous surveys.

The following sections discuss the functions of the D-rings, dosimetry studies at other nuclear power plants, and previous studies performed at Waterford 3.

1.2 Definition and Function of the Biological Shield

The reactor support structure consists of a subterrainean base mat upon which rests reinforced concrete primary and secondary shield walls. These primary and secondary shields walls provide "biological" protection from neutron and gamma radiation originating from the reactor vessel and are commonly called D-rings because from overhead they resemble "D"s. Figures 1-1 to 1-3 (So85) contain an overhead view of the D-rings within the containment structure on the +46 ft., +21 ft., and -4 ft. elevations.

The purpose of the primary shield is to provide support to the reactor vessel and to attenuate the neutron flux exiting the core region. As a result, this shield limits neutron activation of component and structural materials outside the core. In conjunction with the secondary shield walls the primary shield reduces the general area radiation levels to allow access to the reactor coolant system following reactor shutdown. The biological shields also permit limited entry into the containment building while the reactor is at power.

The principal function of the secondary shield wall is to supplement the primary shield in reducing both neutron and gamma dose rates from the reactor core and gamma dose rates from activity within the reactor coolant. The secondary shields also serve the function of supporting the reactor coolant system, which includes the reactor coolant pumps (RCP), coolant piping, and the steam generators (S/G). The terms secondary shield walls and D-rings will be used interchangeably throughout this thesis.

Since the biological shield effectively reduces neutron and gamma

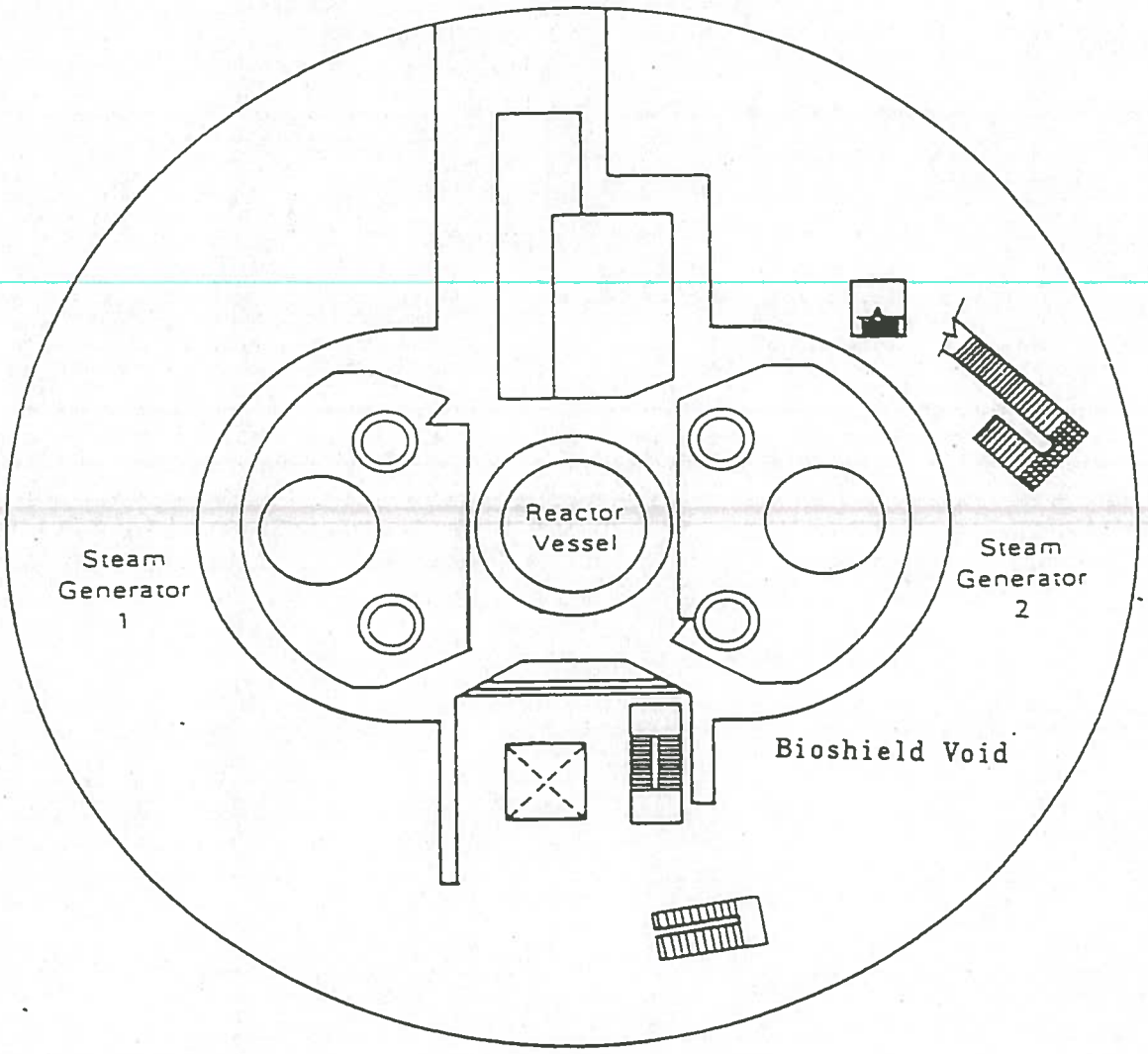

Figure 1-1. Physical Layout of the D-rings Inside the Containment Structure at the -4 ft. Elevation

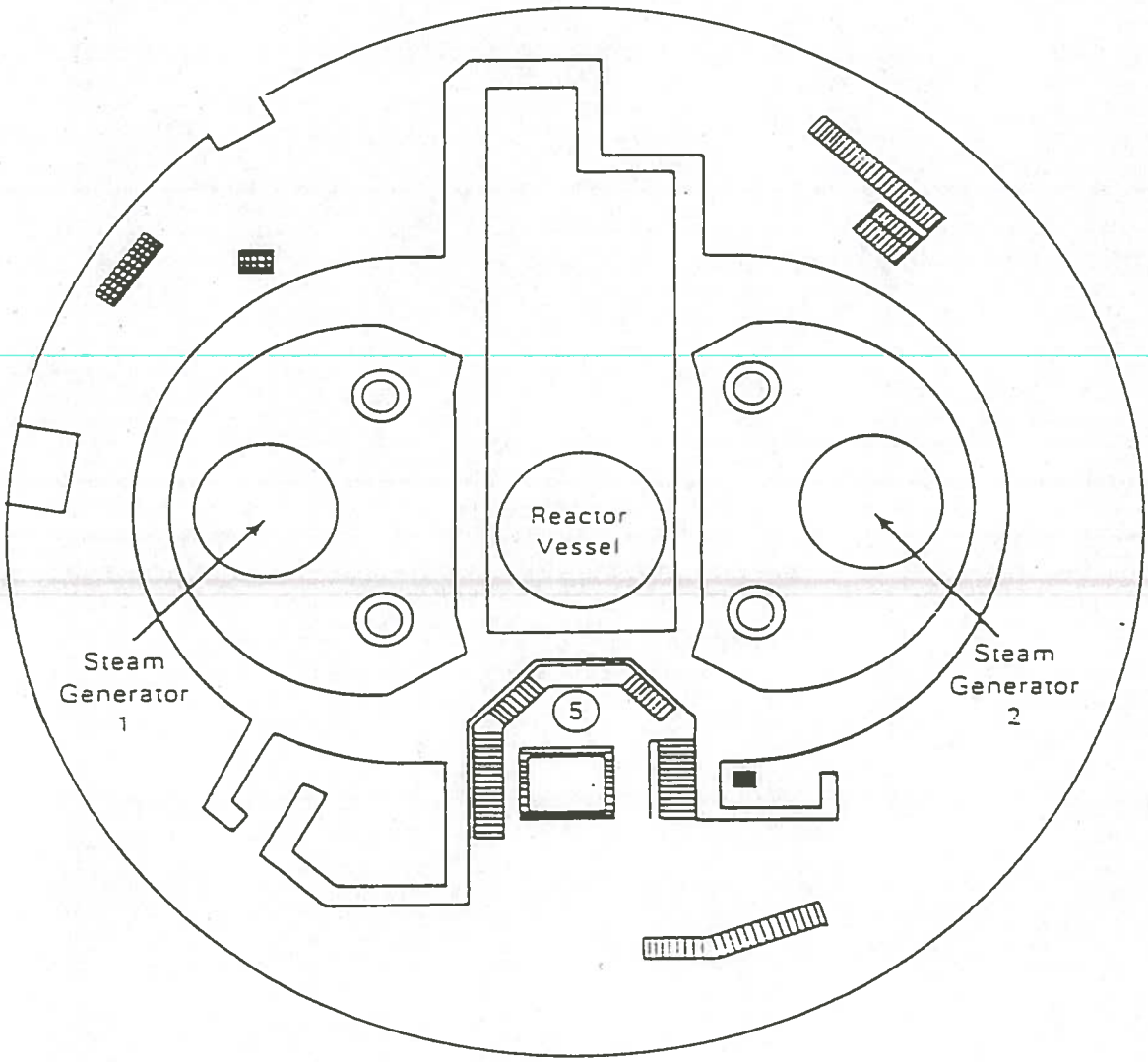

Figure 1-2. Physical Layout of the D-rings Inside the Containment Structure at the +21 ft. Elevation

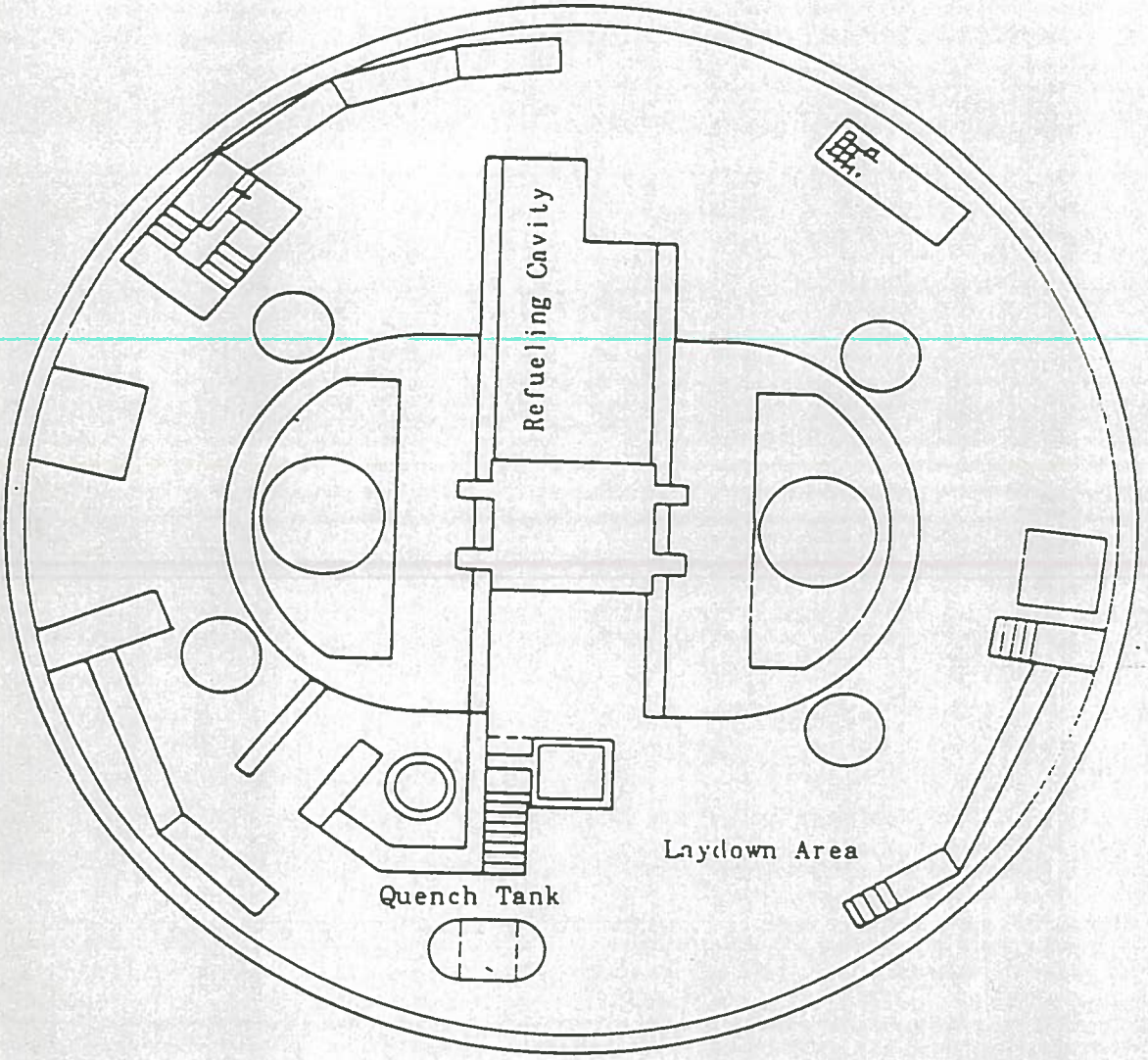

Figure 1-3. Physical Layout of the D-rings Inside the Containment Structure at the +46 ft. Elevation

radiation exposure to personnel outside the D-rings, the unattenuated neutron and gamma dose rates which could be encountered inside the shield are unknown and may be extremely high (e.g. > 100 rem/hr.). A major source of the high neutron and gamma dose rates within the D-rings could be from piping penetrations which lead directly to the reactor vessel. In addition, the limited amount of concrete shielding provided by the primary shield wall may contribute greatly to the dose rates. The reactor coolant system components themselves, the S/G, RCPs, and piping, provide an additional source of gamma dose.

1.3 Studies at Other Nuclear Power Plants

In 1981, Pacific Northwest Laboratory (PNL), published the results of neutron spectral analysis and dosimeter responses to neutron exposures at six commercial power plants (En81). Five of these plants were pressurized water reactors with designs by three different nuclear steam supply system manufacturers. The sixth plant was a boiling water reactor. The goals of this study were: 1) to determine the neutron energy spectra inside containment, and 2) to measure the response of personnel dosimeters that were under development or currently in use at nuclear power plants in order to provide instrument specific calibration factors.

The instruments used for the PNL study were a ^{3}He spectrometer, a Tissue Equivalent Proportional Counter (TEPC), Nuclear Track Emulsion film (NTA), polycarbonate film, CR 39 monomer film, and three designs of TLD Albedo dosimeters. The dose equivalent rates determined by the TEPC and spectra generated by the ^{3}He spectrometer were compared to the

response of the personnel dosimeters to determine the degree of overresponse of the dosimeters. This information was used to interpret the dosimeters' relative response to various components of the neutron spectra. This report demonstrates the similarity of the neutron spectra from plant to plant regardless of the physical layout of containment or reactor type. Tables 1-1, 1-2 and Figures 1-4, 1-5 illustrate the similarity of neutron energy spectra outside biological shield walls from two pressurized water reactors (En81,Ha78). Figures 1-4 and 1-5 suggests that since the neutron spectra found at other nuclear power plants are similar, even though the physical layout may be different, the neutron spectra encountered at Waterford should have a spectral shape much the same as those found at other nuclear plants.

The representative differential neutron energy spectra at each reactor indicated a much larger contribution of thermal and low energy neutrons than high energy neutrons. Additionally, the neutron flux above 500 KeV at various locations around containment for all six plants was low, less than 10 neutrons per centimeter squared per second. Average neutron energies outside the biological shield wall(s) at all of the pressurized water reactors were below 100 KeV.

The response of non-albedo thermoluminescent dosimeters (i.e Panasonic UD-802) has been shown to be highly dependent upon thermal neutrons (0.025-5.0 eV) and less dependent on higher energy neutrons. This dependence of Panasonic 802 dosimeters has been observed as a result of participation in both the Neutron Dosimetry Intercomparison Studies performed at Oak Ridge National Laboratory (Si87) and the University of Michigan (Pl83) as well as studies performed at Waterford 3.

	E(I) (MeV)	Differential Flux ($n/cm^2 \cdot MeV \cdot s$)	Integral Flux	Integral Dose Equivalent	Energy Band (MeV)	Flux ($n/cm^2 \cdot s$)
1	2.07E-07	3.10E+08	1.00E+00	1.00E+00	3.89E-07	1.21E+02
2	5.32E-07	4.34E+07	7.72E-01	9.33E-01	2.69E-07	1.17E+01
3	9.93E-07	7.32E+06	7.50E-01	9.26E-01	7.63E-07	5.59E+00
4	2.10E-06	1.61E+06	7.40E-01	9.23E-01	1.61E-06	2.59E+00
5	4.45E-06	4.65E+05	7.35E-01	9.21E-01	3.42E-06	1.59E+00
6	9.42E-06	1.74E+05	7.32E-01	9.21E-01	7.22E-06	1.26E+00
7	2.00E-05	8.23E+04	7.30E-01	9.20E-01	1.53E-05	1.26E+00
8	4.22E-05	4.73E+04	7.27E-01	9.19E-01	3.23E-05	1.53E+00
9	8.94E-05	3.19E+04	7.24E-01	9.18E-01	6.89E-05	2.20E+00
10	1.89E-04	2.42E+04	7.20E-01	9.17E-01	1.45E-04	3.51E+00
11	4.04E-04	1.96E+04	7.14E-01	9.15E-01	3.18E-04	6.23E+00
12	8.55E-04	1.63E+04	7.02E-01	9.12E-01	6.40E-04	1.04E+01
13	1.80E-03	1.33E+04	6.82E-01	9.07E-01	1.38E-03	1.84E+01
14	3.80E-03	1.01E+04	6.47E-01	8.98E-01	2.91E-03	2.94E+01
15	8.05E-03	6.93E+03	5.92E-01	8.84E-01	6.20E-03	4.30E+01
16	1.70E-02	4.20E+03	5.11E-01	8.64E-01	1.30E-02	5.46E+01
17	3.61E-02	2.23E+03	4.08E-01	8.24E-01	2.77E-02	6.18E+01
18	7.64E-02	1.03E+03	2.91E-01	7.45E-01	5.86E-02	6.04E+01
19	1.58E-01	4.06E+02	1.78E-01	6.09E-01	1.13E-01	4.59E+01
20	3.18E-01	1.30E+02	9.14E-02	4.33E-01	2.27E-01	2.95E+01
21	6.40E-01	3.03E+01	3.58E-02	2.40E-01	4.56E-01	1.38E+01
22	1.29E+00	4.61E+00	9.75E-03	8.74E-02	9.20E-01	4.24E+00
23	2.59E+00	4.40E-01	1.76E-03	1.66E-02	1.85E+00	8.14E-01
24	5.22E+00	2.86E-02	2.22E-04	2.21E-03	3.73E+00	1.07E-01
25	1.05E+01	1.42E-03	2.14E-05	2.24E-04	7.50E+00	1.07E-02
26	1.96E+01	6.22E-05	1.28E-06	1.40E-05	1.09E+01	6.78E-04

Table 1-1. Multisphere Spectrometer Data for Figure 1-4

Table 1-2 Multisphere Spectrometer Data for Figure 1-5

	E(I) (MeV)	Differential Flux ($n/cm^2 \cdot MeV \cdot s$)	Integral Flux	Integral Dose Equivalent	Energy Band (MeV)	Flux ($n/cm^2 \cdot s$)
1	2.07E-07	3.68E+09	1.00E+00	1.00E+00	3.89E-07	1.43E+03
2	5.32E-07	1.83E+09	4.43E-01	7.98E-01	2.69E-07	4.92E+02
3	9.93E-07	4.16E+08	2.52E-01	7.26E-01	7.63E-07	3.17E+02
4	2.10E-06	5.58E+07	1.28E-01	6.77E-01	1.61E-06	8.98E+01
5	4.45E-06	6.75E+06	9.34E-02	6.64E-01	3.42E-06	2.31E+01
6	9.42E-06	8.95E+05	8.44E-02	6.61E-01	7.22E-06	6.46E+00
7	2.00E-05	1.40E+05	8.19E-02	6.60E-01	1.53E-05	1.01E+00
8	4.22E-05	2.68E+04	8.11E-02	6.60E-01	3.23E-05	8.66E-01
9	8.94E-05	6.33E+03	8.07E-02	6.59E-01	6.89E-05	4.36E-01
10	1.89E-04	1.84E+03	8.06E-02	6.59E-01	1.45E-04	2.67E-01
11	4.04E-04	6.60E+02	8.05E-02	6.59E-01	3.18E-04	2.10E-01
12	8.55E-04	2.90E+02	8.04E-02	6.59E-01	6.40E-04	1.86E-01
13	1.80E-03	1.55E+02	8.03E-02	6.59E-01	1.38E-03	2.14E-01
14	3.80E-03	9.97E+01	8.02E-02	6.59E-01	2.91E-03	2.90E-01
15	8.05E-03	7.62E+01	8.01E-02	6.59E-01	6.20E-03	4.72E-01
16	1.70E-02	6.83E+01	7.99E-02	6.59E-01	1.30E-02	7.84E-01
17	3.61E-02	7.04E+01	7.96E-02	6.59E-01	2.77E-02	1.95E+00
18	7.64E-02	8.13E+01	7.88E-02	6.58E-01	5.86E-02	4.76E+00
19	1.58E-01	1.01E+02	7.70E-02	6.56E-01	1.13E-01	1.14E+01
20	3.18E-01	1.23E+02	7.26E-02	6.44E-01	2.27E-01	2.79E+01
21	6.40E-01	1.27E+02	6.17E-02	5.98E-01	4.56E-01	5.79E+01
22	1.29E+00	7.75E+01	3.91E-02	4.34E-01	9.20E-01	7.13E+01
23	2.59E+00	1.44E+01	1.13E-02	1.31E-01	1.85E+00	2.66E+01
24	5.22E+00	6.48E-01	9.72E-04	1.19E-02	3.73E+00	2.42E+00
25	1.05E+01	1.06E-02	3.15E-05	4.05E-04	7.50E+00	7.95E-02
26	1.96E+01	1.05E-04	4.46E-06	6.01E-06	1.09E+01	1.14E-03

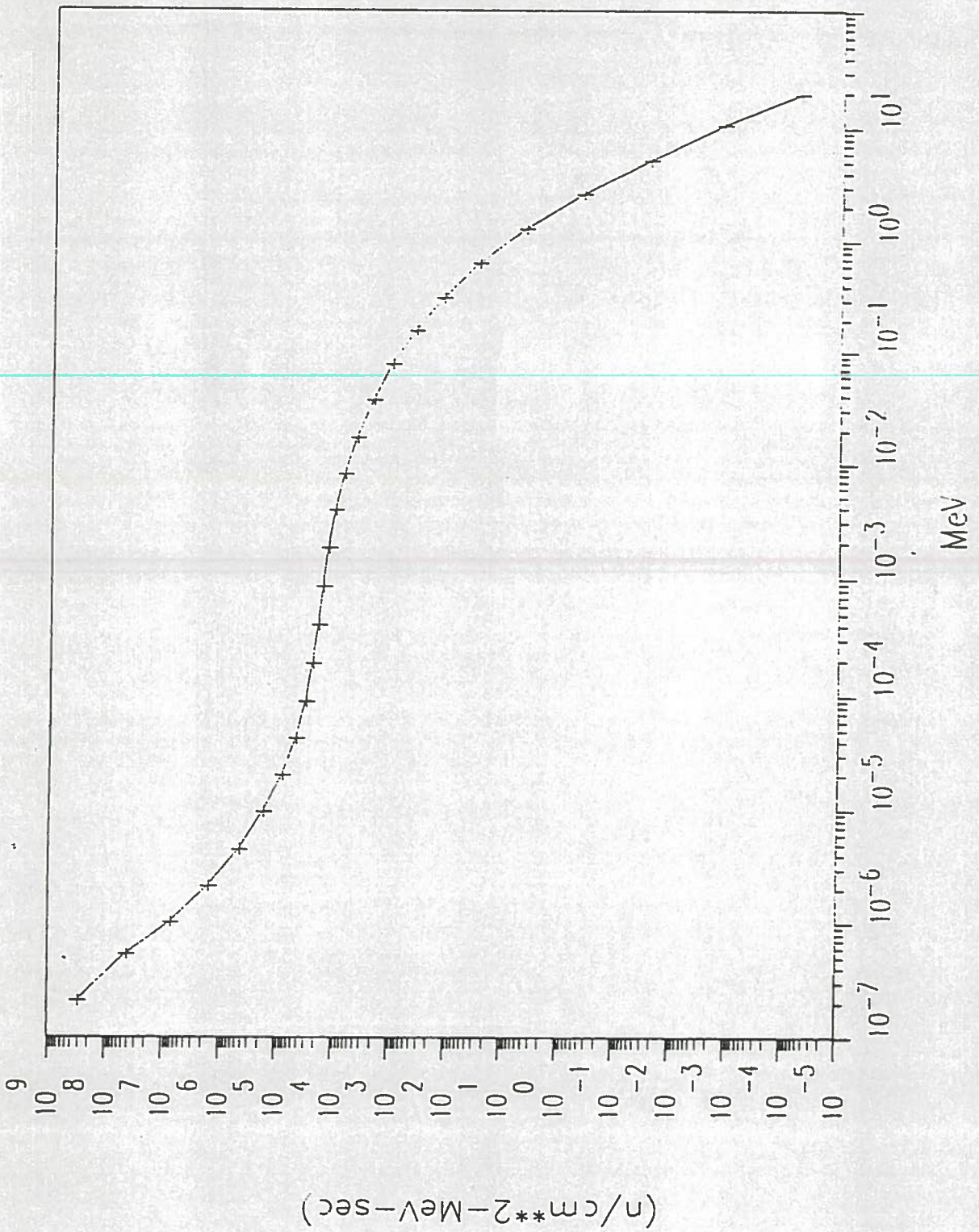

Figure 1-4. Differential Neutron Energy Spectra Outside the Biological Shield at a Pressurized Water Reactor with a Containment Structure Unlike Waterford's (En81)

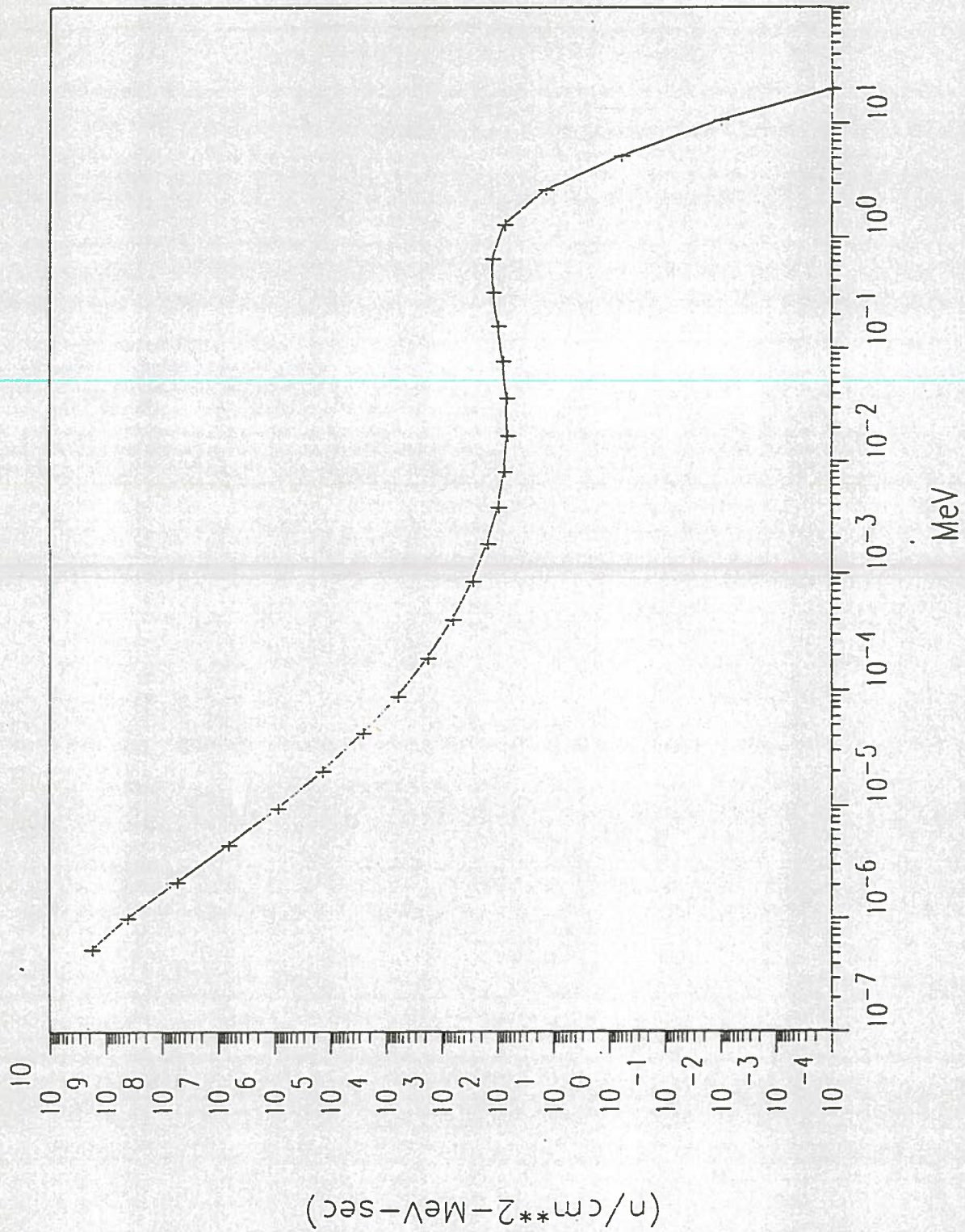

Figure 1-5. Differential Neutron Energy Spectra Outside the Biological Shield at a Pressurized Water Reactor with a Containment Structure Unlike Waterford's (En81)

1.4 Pevious Studies at Waterford 3

Numerous studies have been performed at Waterford to determine the neutron and gamma dose equivalent rates inside containment. These studies have been performed for the dual purposes of providing dosimeter correction factors for the calibration of dosimetry systems and for the quantification of radiation dose rates inside containment.

Battelle-Northwest (So85) conducted a study in April, 1985 on neutron dose equivalent rates and energy spectra inside the containment building during 20 and 50 percent power levels. This study was performed to generate bonner sphere and TLD correction factors specifically for use at Waterford. Although this particular study did not include gamma dose rates, they have been extensively measured and documented (Cl87).

In the Battelle-Northwest study, measurements were made with a tissue equivalent proportional counter (TEPC), ^{3}He spectrometer, and Waterford's portable survey instruments and personnel neutron dosimeters (Panasonic 802 TLDs). The TEPC system was used to measure the actual neutron dose equivalent rates at locations inside containment. The TEPC system is energy independent and directly measures absorbed dose. It converts this absorbed dose into millirem by applying an internally generated quality factor to the measured output. The ^{3}He spectrometer was used to generate a neutron spectrum between 10 KeV and 1 MeV. From Battelle's HESTRIP computer code (En81) and many previous calibration measurements, estimates of thermal, epithermal, and fast components were determined.

Each detector, the TEPC, the ^{3}He spectrometer, the bonner sphere, and the TLDs were placed at predetermined locations on the +46 ft., +21 ft., and -4 ft. elevations inside containment. These elevations inside containment at Waterford are relative to sea level. For example, the +46 level is an elevation inside containment 46 feet above sea level, whereas the -4 elevation is 4 feet below sea level. Figure 1-6 displays a profile view of the elevations inside containment. By comparing the actual dose rate measured by the TEPC to the responses of bonner spheres and TLDs, a device and location specific correction factor was assigned for different locations within containment.

The Battelle study also provided site specific differential neutron energy spectra greater than a 10 KeV threshold and true neutron dose equivalent rates based upon TEPC output. These data were used to produce dose correction factors for both portable bonner spheres and personnel neutron monitors. The bonner spheres, which had been calibrated to a D_2O moderated californium spectrum, overresponded by a factor of 2.1 to 2.4 in the "hardest" spectrum in the survey which was found at the +46 ft. level near the refueling cavity. At other locations on the +46 ft. level the bonner spheres responded high by factors of 3 to 7. The reason for this response is that the californium spectrum is harder (contains a large percentage of high energy neutrons) than spectra found in containment and the bonner sphere is highly thermal neutron sensitive. The personnel dosimeters, which were also calibrated to a D_2O californium spectrum, responded higher than the bonner sphere when exposed to an identical spectrum. The "hard" spectra on the +46 ft level yielded the lowest overresponse with a factor of 5.1 to 5.9. On the +21 ft level the

Figure 1-6. Profile View of Elevations Inside Containment at Waterford

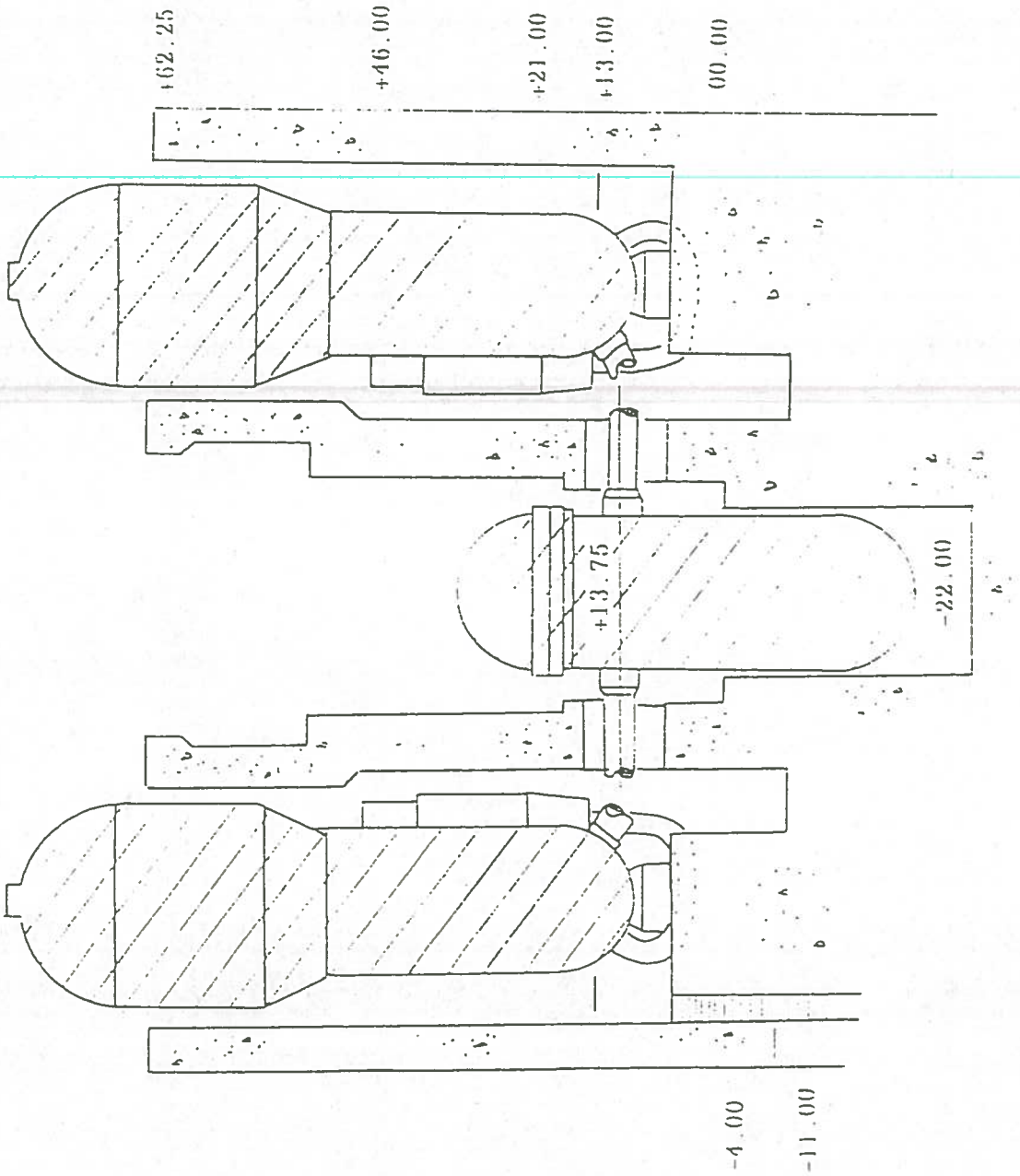

dosimeter overresponse was 6.4 to 11.0. On the -4 ft level the overresponse ranged from 9 to 32. Also noteable is that the average energy throughout containment is less than 100 Kev, and at most locations surveyed, the measurable neutron flux above a 10 KeV threshold was less than 100 neutrons per centimeter squared per second.

A report by Clark (Cl87) compiled the extensive survey data on neutron and gamma dose rates measured inside containment during reactor start-up biological shield surveys and subsequent power entries between 1985 and 1987. The report assumed linear extrapolation of dose rates as a function of power. A compilation of the neutron dose rates was charted for all power levels from 0 to 100 percent power by using the data from these surveys. The biological shield survey data was collected at permanent numbered locations on each elevation in the containment building. The dose rates at each designated power level and measurement point were then transposed from survey maps and recorded in table form to correlate increasing dose rates with increasing power levels. The survey meters used to compile this data were Eberline PNR-4 portable rem counters for neutron dose rates and Eberline RO-2 ion chamber survey meters for gamma dose rates. The battery operated neutron rem counter was used to detect dose equivalent rates over the energy range from 0.025 eV to 10 MeV (Eb88).

The measurements contained in this report demonstrate the varying neutron dose rates with elevation inside the containment building. On the -4 ft. elevation, the highest dose rate measured was 470 mrem/hr neutron at 100% power. This dose rate is at a location below the D-ring and has significant concrete shielding between the measurement location

and the reactor. At the +21 ft. level the maximum neutron dose rate was 515 mrem/hr. Overall the dose rates throughout the +21 ft. elevation are significantly higher than to those taken on the -4 ft. elevation. This increase over the -4 ft. elevation is possibly due to hotleg and coldleg piping leading from the reactor vessel and penetrating through the primary shield into the D-rings. At the +35 ft. level the neutron dose rates decrease, with 400 mrem/hr as the highest measurement on this level. It has been postulated that the dose rates decrease because this elevation is above the direct line of site of primary shield penetrations within the D-rings. On the +46 ft. elevation the dose rates increase significantly. The measured neutron dose rates at the north end of the cavity on the refueling machine were extrapolated to 7.4 rem/hr. The dose rates on the +46 ft. level are the highest, possibly due to both a direct line of sight to the reactor core and backscatter from the annulus.

The report by Clark is a compilation of instrumental survey data. It contains neutron dose rates that are uncorrected instrumental responses, rather than actual dose rates, since the previously generated correction factors (So85) were not applied. Calibration factors for most of these measurment locations have been determined (So85), and by applying the correction factor to meter response at each specific location, actual dose rates can be determined.

1.5 Objectives

The gamma dose rates within the D-rings are calculated by QAD-CG using the reactor vessel and the steam generator as the primary sources of gamma radiation. A three dimensional model of the reactor vessel, the

primary and secondary shield walls, and the reactor coolant system is constructed to represent the D-ring and its components. Since QAD can only do calculations for a single source, both sources of gamma radiation will be modeled and calculated separately and then combined to get a total gamma dose rate.

It has been determined that the Panasonic UD-802 TLD is highly dependent on the neutron energy spectrum (Pl83). Because of the Panasonic's responses to thermal neutrons and the relative quantity of thermal neutrons present, an approximation of the spectra encountered inside the D-rings must be generated. This is accomplished by using limited neutron activation analysis to supplement spectra from the Battelle study (So85). Neutron activation is used to characterize both the thermal component of the neutron energy spectrum and bound the upper limit of the fast neutron component. A neutron energy spectrum from Battelle will be merged with the activation results to form a complete representative spectrum for a location within the D-rings.

Once the neutron spectrum inside the D-rings are approximated, site specific calibration factors for the TLDs within the D-rings will be estimated. Using a correlation of concrete thickness and TLD response calibration factors in areas outside the biological shield can be applied to those areas inside the D-Rings with similar irradiation geometry. Using these data and gamma dose rates calculated by QAD-CG, the neutron plus gamma dose equivalent rates can be estimated.

Chapter 2

CALCULATION OF GAMMA DOSE RATES USING QAD-CG

2.1 Background

QAD-CG (Ca77) is a Point Kernel computer code that calculates gamma ray fluxes, uncollided dose rates, and total dose rates. The first version of QAD was developed by Los Alamos National Laboratory and applied in 1961 (Ma67). Since then, individual modifications have been made to produce codes to suit individual needs. QAD-CG was developed by incorporating the Morse Combinatorial Geometry (St70) subroutines into QAD-P5A to replace the somewhat cumbersome quadratic surface input used in all previous QAD codes. This modification considerably reduces the time requirements for constructing the geometry input.

2.2 Theory of Calculations

The QAD-CG code calculates the dose rate at a detector point for each source energy group with the following formula:

$$\dot{D}_j = \sum_i K_j * \frac{S_{ij}}{4\pi R^2} * e^{-\sum_\kappa (\mu_j t_\kappa)} * B_{j\kappa}$$

where

j = energy group index

i = source point index

κ = region index

K = flux to dose rate
conversion factor (rads/unit flux)

S = source strength (photons/sec)

R = distance from source point to detector (cm)

B = dose buildup factor

μ = total attenuation coefficient (1/cm)

t = total penetration distance (cm)

In general, the code calculates the gamma flux from each source point according to the attenuation and buildup along a straight line path between the source and the detector for each material composition and the distance through each composition. This process is repeated until all source points in the source volume have been calculated. The code then sums the flux in each energy group and converts this flux to dose rate.

The buildup factor, which is always greater than 1, is the ratio of the total intensity of the radiation, including both primary and scattered components, to the intensity of the primary photons. Depending on the scattering medium, buildup factors can increase dose rates significantly, therefore the buildup factors must be considered to calculate a representative dose rate. The buildup factors used in QAD-CG are based on the Goldstein and Wilkens moments method calculations for gamma ray transport in infinite homogeneous media (Go54).

Combinatorial Geometry (CG) enables the user to describe three-dimensional configurations and their material compositions using geometric bodies such as right circular cylinders, spheres, boxes, truncated cones, and arbitrary polyhedrons. These bodies are oriented by

cylindrical, cartesian, or spherical coordinate systems with the center of the source volume placed at the vertex. This combination of shapes forms a geometric model representing the actual situation.

Advantages of QAD-CG not only include the use of CG but also the ability to position many detectors in a single run, and the creation of a standard model which can be modified to suit future needs.

2.3 Reactor Vessel as the Source for QAD Input

Input for QAD-CG consists of describing the source volume, the shielding materials surrounding the source, and the locations of the detector points. The geometric model using the reactor vessel as the source consists of the reactor vessel, the reactor coolant system, and the primary and secondary shields.

In order to calculate gamma dose rates inside the D-rings all of the sources had to be considered. Sources producing gamma radiation are the reactor vessel (RV), and the steam generator (S/G). The main source of photons originating from the reactor vessel region are capture gammas resulting from leakage neutrons. Prompt fission photons, fission products, activation products, and capture gammas from leakage neutrons contribute to gamma fluxes exiting the reactor region. In the reactor coolant, fission products, activation products, and ^{16}N provide the gamma ray source. Theoretically, fission products should not enter the reactor coolant but due to failed fuel cladding mixed fission products escape into the coolant system. Because QAD-CG can only calculate one source at a time, the RV and the S/G, were modeled separately.

Description of the RV source was taken from Waterford's Final Safety

Analysis Report (FSAR88). Table 2-1 lists the gamma flux opposite the RV at full power according to the upper limit gamma energy. Since QAD-CG calculates the dose rate with the gamma energy in MeV/sec, each energy group flux was multipied by the surface area of the RV and the energy of group, to produce the source strength in MeV/sec. This source strength represents the integrated source emerging from the vessel. The total source is then distributed uniformly throughout the volume of the reactor that produces the majority of gamma flux. The volume used in the calculation of the vessel source strength was the active region of the fuel assemblies (14 ft.) within the reactor vessel. Table 2-1 lists the gamma fluxes for the top, bottom, and side of the RV. Since the top and bottom of the reactor employs sufficient shielding materials (i.e., control mechanisms on top and concrete on bottom) only the gamma fluxes on the side was used in the source representation of the RV. Axial variation of the fluxes along the side of the vessel was not taken into consideration due to the relative height of the vessel compared to the region of the vessel modeled.

Once representation of the source was completed, the dimensions and material compostion of the the shielding bodies surrounding the RV had to be modeled. These bodies include the primary shield, the secondary shield, penetrations through the secondary shield, hotleg and coldleg piping, RCPs, and S/G.

The origin of the model is located at the bottom of the RV and dimensions for all bodies are taken from this reference point. Since the gamma fluxes are specified on the outside of the RV, the material composition of the RV is assumed to be air which provides minimal self

Table 2-1. Gamma Fluxes Outside the Reactor Vessel at Full Power Operation from FSAR*

Upper Limit Energy (MeV)	Side	Top	Bottom
10.00	3.05E+7	3.92E+2	7.34E+3
9.00	2.62E+8	2.90E+3	1.08E+7
8.00	4.97E+8	3.08E+3	1.93E+7
7.00	5.40E+8	5.18E+3	3.42E+7
6.00	5.99E+8	6.33E+3	4.91E+7
5.00	7.40E+8	8.03E+3	6.71E+7
4.00	9.45E+8	1.05E+4	8.88E+7
3.00	1.40E+9	1.37E+4	1.25E+8
2.00	2.51E+9	2.00E+4	1.94E+8
1.38	1.14E+9	1.21E+4	1.14E+8
1.00	8.23E+8	1.08E+4	1.07E+8
0.75	1.96E+9	1.49E+4	1.51E+8
0.25	3.79E+9	2.95E+4	3.21E+8

*All fluxes in (γ/cm^2-sec)

shielding. The primary and secondary shield walls are ordinary concrete. The S/G is assumed to be low density inconel (an alloy consisting mainly of nickel, chromium, and iron) , and the RCPs are modeled as high density inconel. The penetrations through the D-rings for coolant piping are assumed to be air, and the hotleg and coldleg pipes are modeled as water surrounded by 0.5 inches of steel. Figure 2-1 shows a two-dimensional sketch of the geometric model constructed with the reactor vessel as the source. Appendix A contains the input for this particular model.

2.4 Steam Generator Hotleg Plenum Source

The geometric model for the S/G as the source entailed calculations of the activity in residing within the coolant. Referring to Figure 2-2 (NSSS82), the S/G is divided into a primary and secondary loop to produce the steam necessary for electrical output. The primary loop consists of coolant flowing into the S/G via the hotleg plenum then through the tubing and back out the coldleg. The secondary loop provides feedwater which flows around the primary loop tubing. The coolant flowing through the primary loop of the tubing comes directly from the reactor core, and carries fission products from leaking fuel, and activation products formed by neutron bombardment of suspended particulate materials within the coolant. Also taken into consideration was the fast neutron activation of oxygen in the coolant. Activation of the oxygen produces ^{16}N which emits high energy gamma rays. The coolant in the primary loop is a significant source of gamma radiation inside the D-rings.

The S/G source was further divided into two components. The first

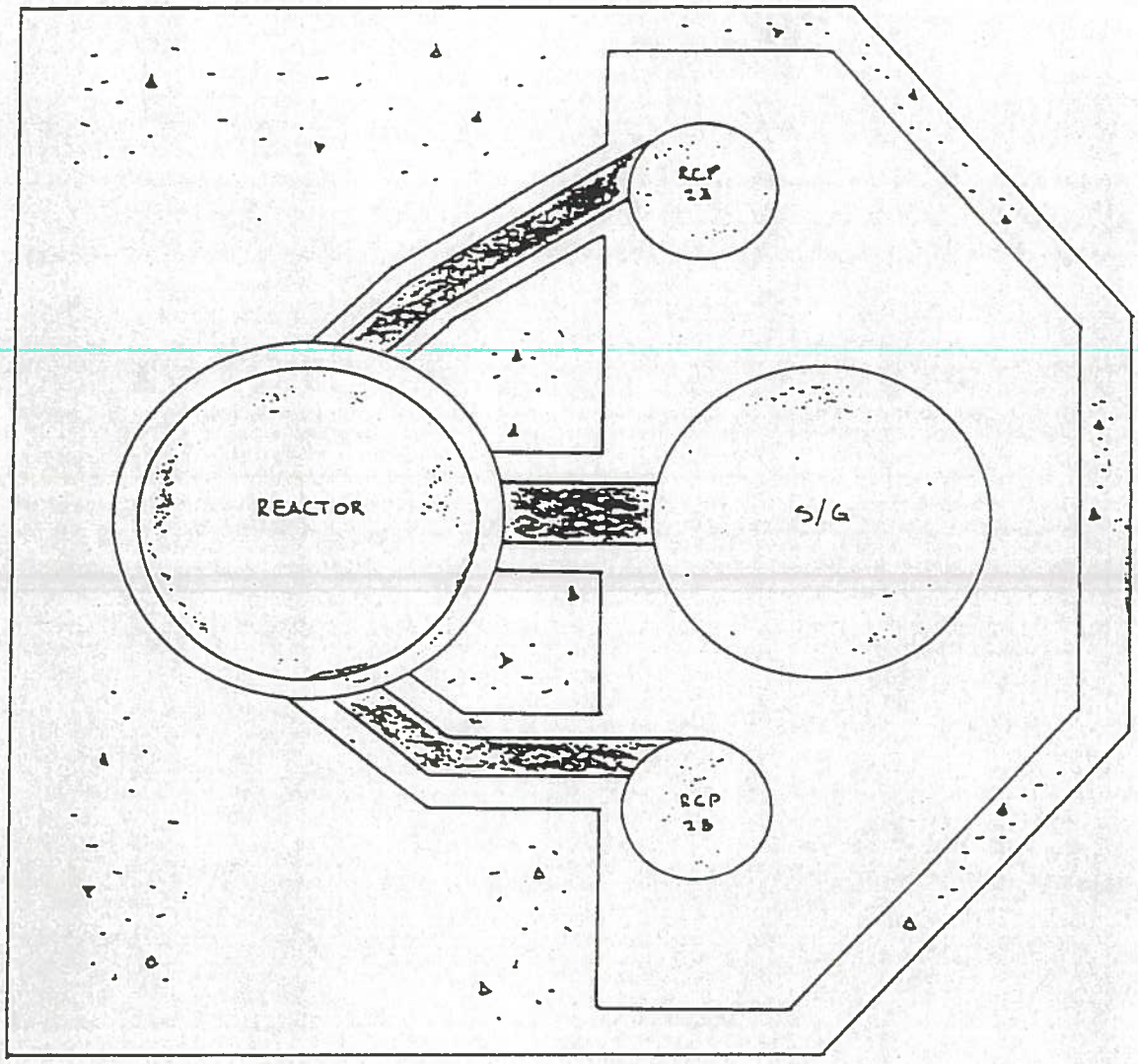

Figure 2-1. Two Dimensional Sketch of Geometric Model with the Reactor Vessel Source

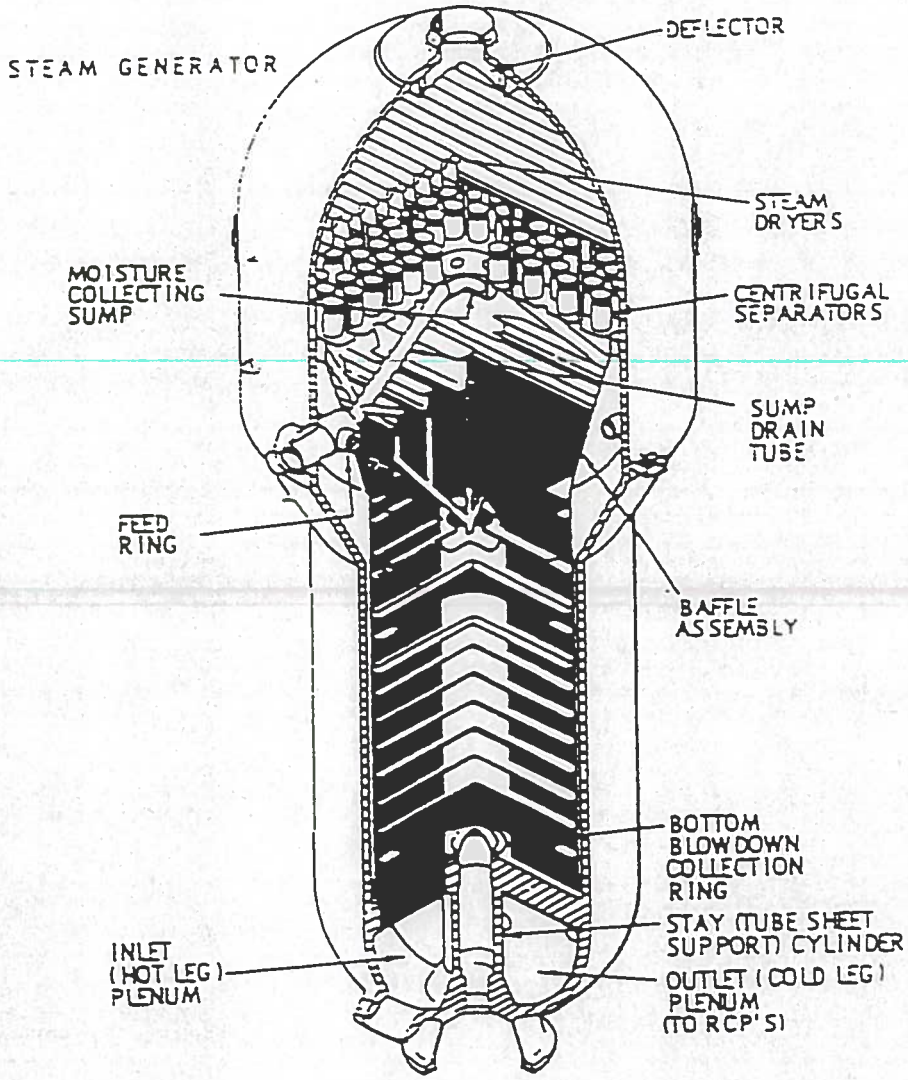

Figure 2-2. Steam Generator Provided by NSSS

reason for this division is a result of differing self shielding provided by each component. The hotleg plenum contains only coolant to provide self shielding. The tubing section of the S/G is made up of mostly inconel and as a result provides relatively more self shielding. Another reason for dividing the S/G is the size of the sources. The total volume of the hotleg plenum is small compared to the tubing section. For these reasons, the two components are modeled separately.

Waterford's Final Safety Analysis Report (FSAR88) lists the average reactor coolant radionuclide concentration in μCi/ml for each nuclide; these data were used to calculate the activity in the hotleg plenum. By calculating the volume of coolant inside the plenum, a total activity of each nuclide in Curies and MeV/sec could be estimated. The computer program MICROSHIELD (Mi87) was used to determine the gamma spectrum for each nuclide. By examining the gamma dose rate produced by one curie of activity, the most significant energy group contributing to the dose rate could be determined. This is the gamma energy utilized for representation of each nuclide.

The coolant concentration of ^{16}N was calculated based on the flux at the reactor vessel outlet and decay corrected from the time leaving the reactor vessel to the time it reaches the hotleg plenum, or middle of the tubing. Table 2-2 lists all of the nuclides, the gamma energies used, their concentrations, and activities. The nuclides were then grouped by energy for input into QAD-CG. These energy groups ranged from 0.01 to 6.5 MeV. Appendix D contains the different energy groups and the nuclides contained in each group.

The geometric bodies included in this model consist of the S/G,

Table 2-2. Steam Generator Activity by Nuclides In The Hotleg Plenum

Nuclide	Energy (MeV/dis)	μCi/ml	Curies	MeV/sec
^{51}Cr	0.320	3.610E-3	0.0286	3.319E+7
^{54}Mn	0.834	5.934E-4	0.0047	1.451E+8
^{59}Fe	1.292	1.901E-3	0.0151	3.138E+8
^{58}Co	0.811	3.050E-2	0.2417	7.207E+9
^{60}Co	2.500	3.830E-3	0.0303	2.807E+9
^{239}Np	0.277	2.120E-3	0.0168	1.260E+7
^{83}Br	0.529	6.450E-3	0.0511	9.815E+8
^{86}Rb	1.077	1.512E-4	0.0012	4.168E+6
^{89}Sr	0.909	6.670E-4	0.0053	1.653E+4
^{91}Y	1.205	3.810E-3	0.0302	4.038E+6
^{99}Mo	0.140	8.020E-1	6.3550	1.482E+9
^{99m}Tc	0.141	5.440E-1	4.3110	1.994E+11
^{127m}Tc	0.057	5.350E-4	0.0042	4.698E+4
^{127}Tc	0.418	1.270E-3	0.0101	1.540E+6
^{129m}Te	0.696	2.660E-3	0.0211	1.661E+7
^{129}Te	0.028	2.090E-3	0.0165	2.567E+6
^{130}I	0.536	3.241E-3	0.0256	5.041E+8
^{131m}Te	0.773	4.190E-3	0.0332	7.223E+7
^{131}I	0.364	5.070E-1	4.0170	4.388E+10
^{132}Te	0.228	4.650E-2	0.3685	2.738E+9
^{132}I	0.667	1.340E-1	1.0620	4.926E+9
^{133}I	0.529	6.190E-1	4.9050	6.866E+10

Table 2-2. Steam Generator Activity by Nuclides In The Hotleg Plenum (continued)

Nuclide	Energy (MeV/dis)	μCi/ml	Curies	MeV/sec
^{134}I	0.847	6.090E-2	0.4826	1.430E+10
^{134}Cs	0.605	4.470E-2	0.3542	7.735E+9
^{135}I	1.260	2.750E-1	2.1290	2.906E+10
^{136}Cs	1.048	2.270E-2	0.1799	4.447E+9
^{137m}Ba	0.667	2.020E-2	0.1601	3.547E+9
^{83m}Kr	0.009	2.654E-2	0.2103	4.096E+6
^{85m}Kr	0.152	1.392E-1	1.1031	4.646E+9
^{85}Kr	0.514	2.896E-1	2.2950	4.347E+10
^{87}Kr	0.403	7.582E-2	0.6008	4.429E+9
^{88}Kr	2.392	2.529E-1	2.0040	6.137E+10
^{89}Kr	0.586	6.314E-3	0.0500	1.084E+7
^{131m}Xe	0.164	1.534E-1	1.2160	7.371E+9
^{133m}Xe	0.233	2.844E-1	2.2540	1.944E+10
^{133}Xe	0.081	2.392E+1	189.50	2.102E+11
^{135m}Xe	0.787	1.642E-2	0.1301	3.057E+9
^{135}Xe	0.249	4.439E-1	3.5170	2.926E+11
^{137}Xe	0.455	1.137E-2	0.0901	1.518E+7
^{138}Xe	2.016	5.557E-2	0.4403	4.409E+9
^{16}N	6.129	3.582E+1	242.67	2.531E+12

Total Activity: 470.9 Curies

CPs, and the D-ring surrounding them. Because the reactor vessel is modeled seperatly and is not contained within the D-rings, it is not included in this model. Refer to Figure 2-3 for an illustration of this model. The S/G material composition consisted of the hotleg plenum assumed to be all water, the tubing section of the S/G was assumed as 75% Inconel, 25% water, and the top portion as low density (approximately 5.0 grams per square centimeter) steel. The RCPs were modeled as pure Inconel, and the D-rings as ordinary concrete. Appendix C contains the input for this particular model.

2.5 Steam Generator Tubing Source

The third phase of QAD was to model the S/G tubing as a single source. Calculation of the activity of the coolant inside the tubing was identical to that of the S/G hotleg plenum with the exception of having a larger volume of coolant. Table 2-3 lists the gamma energy, the concentration, the activity, and the strength of each nuclide. The only other change in input came from homogenizing the inconel and water of the tubing to produce self shielding. The hotleg and coldleg plenum were modeled as ordinary water. All of the other geometric figures and material compositions remained the same as that for the S/G hotleg plenum. The illustration used for the S/G hotleg plenum can also be applied for this particular model. Appendix E lists the nuclides, their concentrations, activities, and strengths used as input for this particular model.

Table 2-3. Activity by Nuclides in the Steam Generator Tubing

Nuclide	Energy (MeV/dis)	μCi/ml	Curies	MeV/sec
^{51}Cr	0.320	3.610E-3	0.2419	2.807E+8
^{54}Mn	0.834	5.934E-4	0.0347	1.084E+9
^{59}Fe	1.292	1.901E-3	0.1273	3.428E+9
^{58}Co	0.811	3.050E-2	2.0440	6.095E+10
^{60}Co	2.500	3.830E-3	0.2566	5.920E+10
^{239}Np	0.277	2.120E-3	0.1420	1.066E+8
^{83}Br	0.529	6.450E-3	0.4322	8.262E+9
^{86}Rb	1.077	1.512E-4	0.0101	3.522E+7
^{89}Sr	0.909	6.670E-4	0.0447	1.398E+5
^{91}Y	1.205	3.810E-3	0.2553	3.410E+7
^{99}Mo	0.140	8.020E-1	53.734	1.250E+10
^{99m}Tc	0.141	5.440E-1	36.448	1.680E+12
^{127m}Tc	0.057	5.350E-4	0.0358	3.969E+5
^{127}Tc	0.418	1.270E-3	0.0851	1.303E+7
^{129m}Te	0.696	2.660E-3	0.1782	1.404E+8
^{129}Te	0.028	2.090E-3	0.1400	2.240E+7
^{130}I	0.536	3.241E-3	0.2171	4.260E+9
^{131m}Te	0.773	4.190E-3	0.2807	6.120E+8
^{131}I	0.364	5.070E-1	33.969	3.711E+11
^{132}Te	0.228	4.650E-2	3.1155	2.320E+10
^{132}I	0.667	1.340E-1	89.780	4.165E+11
^{133}I	0.529	6.190E-1	41.473	5.810E+11

Table 2-3. Activity by Nuclides in the Steam Generator Tubing (continued)

Nuclide	Energy (MeV/dis)	μCi/ml	Curies	MeV/sec
^{134}I	0.847	6.090E-2	4.0809	1.221E+11
^{134}Cs	0.605	4.470E-2	2.9950	6.540E+10
^{135}I	1.260	2.750E-1	18.425	2.457E+11
^{136}Cs	1.048	2.270E-2	1.5209	4.603E+10
^{137m}Ba	0.667	2.020E-2	1.3530	2.991E+10
^{83m}Kr	0.009	2.654E-2	1.7780	3.465E+7
^{85m}Kr	0.152	1.392E-1	34.682	1.459E+11
^{85}Kr	0.514	2.896E-1	19.405	3.675E+11
^{87}Kr	0.403	7.582E-2	5.0799	3.746E+10
^{88}Kr	2.392	2.529E-1	16.945	5.187E+11
^{89}Kr	0.586	6.314E-3	0.4231	9.169E+6
^{131m}Xe	0.164	1.534E-1	10.280	6.234E+10
^{133m}Xe	0.233	2.844E-1	19.050	1.644E+11
^{133}Xe	0.081	2.392E+1	1602.6	1.770E+12
^{135m}Xe	0.787	1.642E-2	1.1001	2.585E+10
^{135}Xe	0.249	4.439E-1	29.740	2.474E+11
^{137}Xe	0.455	1.137E-2	0.7618	1.284E+8
^{138}Xe	2.016	5.557E-2	3.7232	3.416E+10
^{16}N	6.129	3.582E+1	2049.9	2.138E+13

Total Activity: 4089 Curies

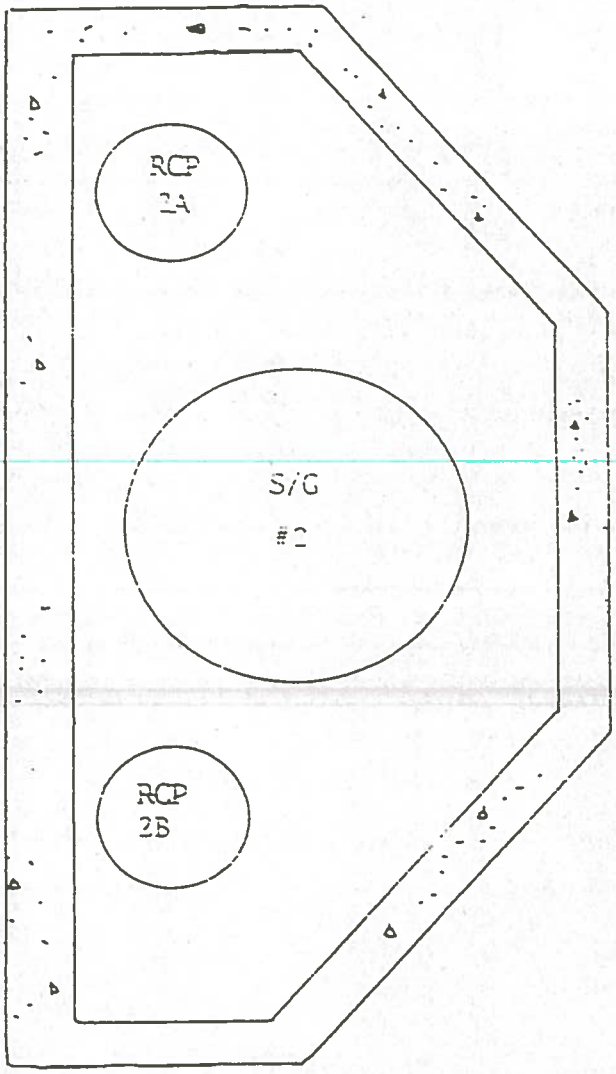

Figure 2-3. Two Dimensional Sketch of Geometric Model with Steam Generator Source

Chapter Three

DETERMINATION OF NEUTRON DOSE EQUIVALENT RATES

For the purpose of personnel dosimetry systems, most neutron spectral surveys conducted at nuclear power plants are instrumental surveys. These surveys are performed to determine neutron energy spectra at specific sites inside containment in order to calibrate portable instruments and thermoluminescent dosimeters. Using the present technology, the instrumentation necessary to determine neutron spectra is typically large, bulky, and requires extensive time and effort for spectral determination. Normally these instruments are temperature sensitive and are not designed for extensive operation in areas where the neutron flux is greater than 1.0E+4 neutrons per centimeter squared per second (En81). As a result, these instruments can lose some of their reliability if not maintained periodically during operation.

Considerations for personnel exposures become significant when quantifying an unknown radiation field inside the containment of a pressurized water reactor (PWR). As a result of extreme temperatures (over 120 degrees F) and measurement locations up to 70 feet above ground level, personnel safety is also important. It was for all these reasons that neutron activation was chosen to characterize the thermal component of the neutron energy spectrum, and bound the high energy component of the spectrum inside the D-rings. Together with previous ^{3}He spectrometer measurements outside the D-rings, this spectra was used to generate TLD correction factors. The remainder of this chapter defines the

methodology for determing appropriate TLD correction factors for use inside the D-rings.

3.1 Activation Packets

The neutron activation packets were prepared in the health physics department counting room at Waterford. All of the materials used in the packets were supplied by the utility with the exception of the indium, which was supplied by the LSU Nuclear Science Center. The packets consisted of both activation samples and TLDs. While the activation materials were present to assist in spectral evaluation, the TLDs were in the packets for determination of neutron dose equivalent rates.

Six activation packets were prepared. In addition, a packet at the #2B RCP ladder which had been distributed in a previous survey (Es88) inside the D-rings but had not been removed was included in this study. Table 3-1 provides a complete description of the contents, weights, TLD identification numbers, and packet locations within the D-rings.

Referring to Table 3-1, most of the activation samples were in the form of foils. The bare gold in each packet was a 0.001 inch strip folded into a small volume to be placed inside cadmium covers. In addition, a gold strip in packet one was used to calculate an estimated geometry self depression correction factor. The cadmium covers are two small covers that encapsulate the gold samples as well as serving as an activation target material itself. The NaCl salt samples were in tablet form, and the indium targets were small cadmium covered foils for three packets and large cadmium covered foils for the remaining three packets. The large volume indium samples were incorporated in order to reduce the threshold of detection to the expected neutron fluence levels. As a

Table 3-1. Weights, Contents and Location of each Activation Packet

Packet #1

Element	Weight
Bare Au	1.108g
Cd - Au	1.053g
Na	15.54g
In volume	2.001g
In foil	550.8mg
Cd cover	4.929g
Au strip	1.054g

TLDs 11907, 11706

Packet #2

Element	Weight
Bare Au	1.060g
Cd - Au	1.091g
Na	15.52g
In volume	2.001g
In foil	629.9mg
Cd cover	3.677g

TLDs 11044, 12562

Packet #3

Element	Weight
Bare Au	1.093g
Cd - Au	1.098g
Na	15.13g
In volume	2.000g
In foil	622.8mg
Cd cover	3.913g

TLDs 15092, 15335

Packet #4

Element	Weight
Bare Au	1.105g
Cd - Au	1.109g
Na	15.45g
In volume	1.996g
In foil	30.65mg
Cd cover	3.808g
Au strip	1.054g

TLDs 15313, 14629

Packet #5

Element	Weight
Bare Au	1.026g
Cd - Au	1.077g
Na	15.56g
In volume	1.990g
In foil	30.09mg
Cd cover	4.458g

TLDs 14434, 115709

Packet #6

Element	Weight
Bare Au	1.100g
Cd - Au	1.076g
Na	15.45g
In volume	1.996g
In foil	30.94mg
Cd cover	4.458g

TLDs 15748, 15756

Packet #	Location
1	1B RCP Ladder
2	S/G #1 Hotleg
3	S/G #2 Hotleg
4	S/G #2 Platform
5	S/G #1 Platform
6	Reactor Cavity

result of errors created by self shielding in both activation and counting, these samples were therefore qualitative rather than explicitly quantitative.

Each activation sample was put into a small plastic bag and joined with duct tape. The samples were double bagged to prevent the sample from getting contaminated during irradiation due to both airborne and smearable radioactive material present in containment. The activation packets were then taped such that one sample was clear of the next so that they would not shield each other during irradiation. After preparation of the packets, they were approximately 1.5 feet long and about 4 inches wide. Rope was then tied to the packets as a means of hanging them in their respective locations within the D-rings.

3.2 Distribution of Packets in Containment

In order to limit personnel radiation exposure, the activation packets were mounted at the selected locations when the reactor was not in operation. On November 13, 1988 a containment entry was made. The reactor had been shut down to perform work on one of the steam generators. A Radiation Work Permit was generated for mounting the packets and required the use of anti-contamination clothing to enter containment and perform work. Some of the packets were hung directly from railings on the top of the D-rings while others had to be positioned using "trot" lines tied to the railings on top of the D-rings. Precautions had to be taken so that the ropes holding the packets would not be pulled into operating equipment and located so that they did not interfere with personnel working on the steam generator. Packet shielding due to components within the D-rings was also an important

factor that had to be taken into account. Figure 3-1 illustrates an elevated view of the activation packets inside the D-rings. The D-rings contain a great deal more equipment than is shown in Figure 3-1. It is this equipment which creates the previously mentioned shielding problems.

In order to simplify calculation of neutron flux, the target nuclides should be allowed to reach saturation activity. As such, the activation packets were left inside the D-rings until all of the activation products had reached saturation. Since ^{24}Na has the longest half-life of the irradiated species (15.06 hrs), it was determined that the packets should be left in the D-rings for at least 3.5 days at full power.

On December 8, 1988 the activation packets were removed from containment following a reactor trip from full power. During the irradiation period, 20.4 effective full power days were generated. The packets were brought to the health physics department counting room and analyzed via gamma spectroscopy.

3.3 Panasonic UD-802 TLD

Waterford 3 uses a Panasonic UD-802 TLD for personnel monitoring. The 802 is the most popular Panasonic model presently in use at most nuclear power plants in the United States due to its sensitivity to beta, gamma, and neutron radiation and the simplicity of its analysis and dose conversion. The 802 TLD contains four elements. Table 3-2 lists the element composition, filtration, and radiation response.

The primary objective of personnel dosimetry is to measure dose equivalent, in units of mrem, at specific depths in tissue. The depths

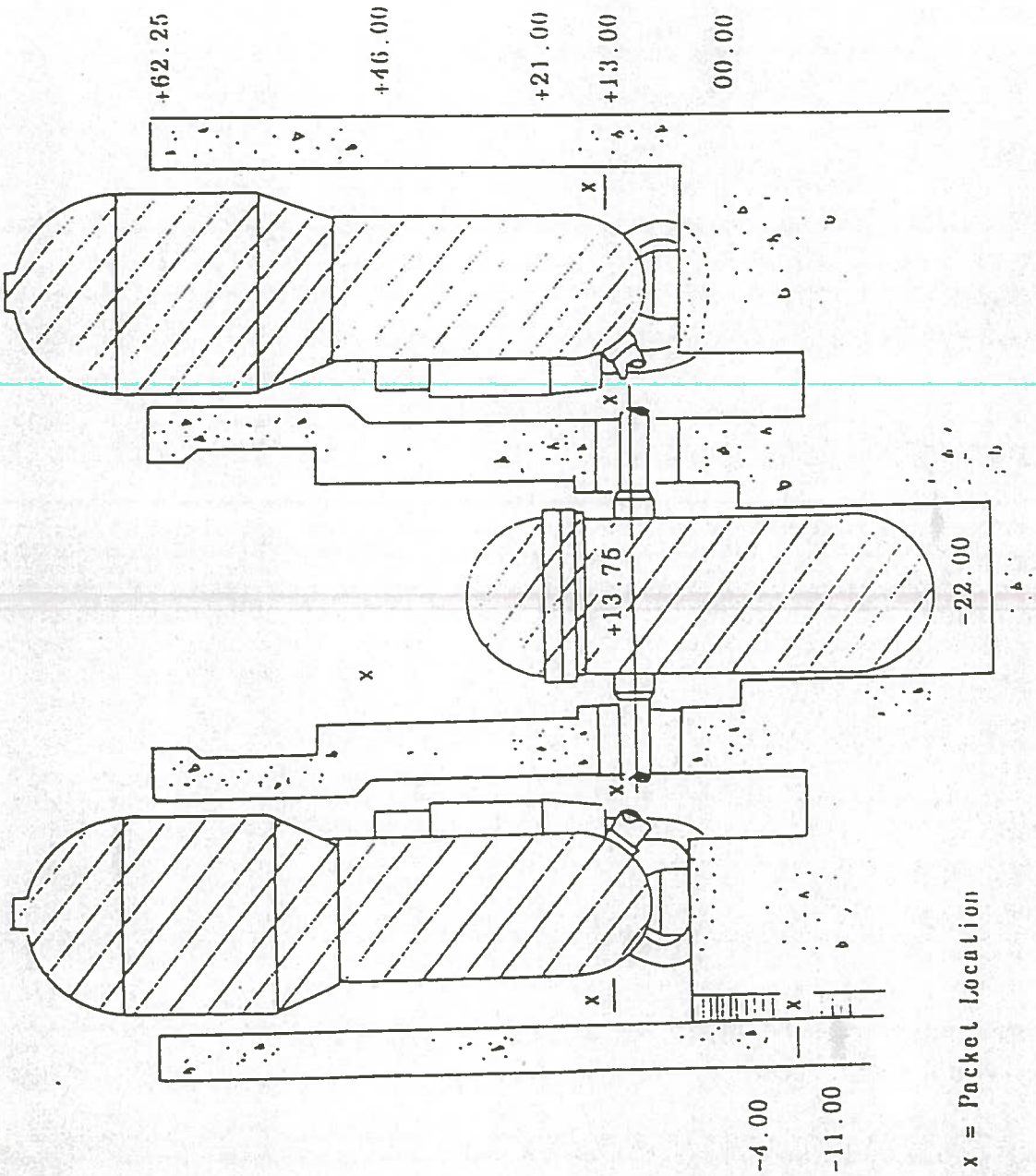

Figure 3-1. Profile View of Location of Activation Packets Inside the the D-rings

Table 3-2. Element Composition, Filtration, and Radiation Response of the Panasonic UD-802 TLD

Element	Phosphor	Filtration (mg/cm^2)	Radiation Response
E1	LiBO	14	beta, gamma, neutron
E2	LiBO	300	gammma, neutron
E3	CaSO	300	gamma
E4	CaSO	1000	high energy gamma

of interest are those corresponding to the beginning of living skin, the depth of the lens of the eye, and the deep dose to red bone marrow. These depths are represented in the 802 by filtrations of 14 mg/cm^2 for skin dose, 300 mg/cm^2 for eye dose, and 1000 mg/cm^2 for the deep dose.

The 802 will respond to beta, photons, and neutron radiation. Element 1 (E1) and element 2 (E2) are $Li_2B_4O_7$:Cu (LiBO) phosphors which are approximately tissue equivalent. Element 1 responds to beta, photons, and neutrons. Element 2, because of shielding, responds mainly to neutron and gamma radiation and high energy beta particles which are capable of penetrating the 300 mg/cm^2 filter. Element 3 (E3) and Element 4 (E4) are $CaSO_4$:Tm (CaSO) phosphors that are not tissue equivalent but have the advantage of very high sensitivity to photons only. Element 3 is sensitive to both high and low energy photons, while E4 responds to high energy photons only due the 1000 mg/cm^2 filtration.

The dominant mode of interaction for thermal neutrons in a TLD is by the process of nuclear capture. A particularly useful type of capture is one that results in the production of an alpha particle. Two of the most common elements in a TLD which are used to detect thermal neutrons by the production of alpha particles are lithium (Li) and boron (B). The thermal neutron cross section for ^6Li is 953 barns and for ^{10}B it is 3840 barns. Since ^6Li and ^{10}B are both present in large amounts in natural $Li_2B_4O_7$:Cu, E1 and E2 of the 802 are high efficiency detectors of thermal neutrons. For determination of the neutron response the gamma response of these elements must be known. The deep dose gamma response (E4) can

be extracted from the E2 response to determine neutron response. This correlation is valid provided there are few high energy beta particles and the ratio of neutron to gamma response is greater than 1:1. For neutron plus gamma response, E2 is used. Therefore neutron reponse is determined by E2 minus E4.

The TLD reader used at Waterford is the Panansonic UD 710. The UD 710 is an automatic reader which uses an optical heating method to liberate energy stored in the traps of the thermoluminescent material. The UD-710 converts light output from a photomultiplier tube to units of mR*. If a TLD reader is calibrated to a given photon source (e.g. ^{137}Cs), then mR* displayed on the reader will correspond to mR delivered by that source. However, for other sources, mR delivered to a TLD may not correspond to mR* displayed because of other types of radiation absorbed by LiBO or CaSO elements, and because CaSO is not tissue equivalent. Therefore the mR* values displayed on the Panasonic TLD reader should not be assumed to be actual milliroentgens, millirem, or millirad.

3.4 Derivation of Neutron Factors for the Panasonic UD-802 TLD

In order to convert neutron response to dose equivalent, the corrected element readings of the Panasonic 802 TLD must be treated by an algorithm. Waterford has developed several algorithms for determination of dose from their TLDs. The particular algorithm of interest is the algorithm specifically designed for the Panasonic 802 TLD - the UD802.ALG. This algorithm was generated as part of the National Voluntary Laboratory Accreditation Program (NVLAP) accreditation process

(ANSI83). This algorithm is contained in Figure 3-2. The algorithm has two major functions which must be completed in sequential order to determine the correct dose equivalent when the radiation type and delivered dose is unknown. First, the algorithm must identify the type of radiation the TLD was exposed to, and second determine the dose equivalent to specified depths in tissue (eye, skin, and deep dose).

The algorithm is divided into three sections; a branch for photons, beta plus gamma, and gamma plus neutron. The neutron plus gamma branch is the one used for evaluation of the TLD's exposed inside the D-rings. The main disadvantage of this algorithm branch is that it cannot distinguish the energy of the neutrons interacting with the dosimeter. A neutron factor (NF) is used to convert from dosimeter response (mR*) to dose equivalent (mrem). The neutron factor is defined mathematically by the following expression:

$$NF = \frac{\int_0^\infty H_D(E)\ \phi(E)\ dE}{\int^\infty H_R(E)\ \phi(E)\ dE}$$

where:

$H_D(E)$ = the time dependent flux to dose conversion function for tissue

$H_R(E)$ = the energy dependent dose response function of the TLD

$\phi(E)$ = the differential flux spectrum representation of the specific environment of interest

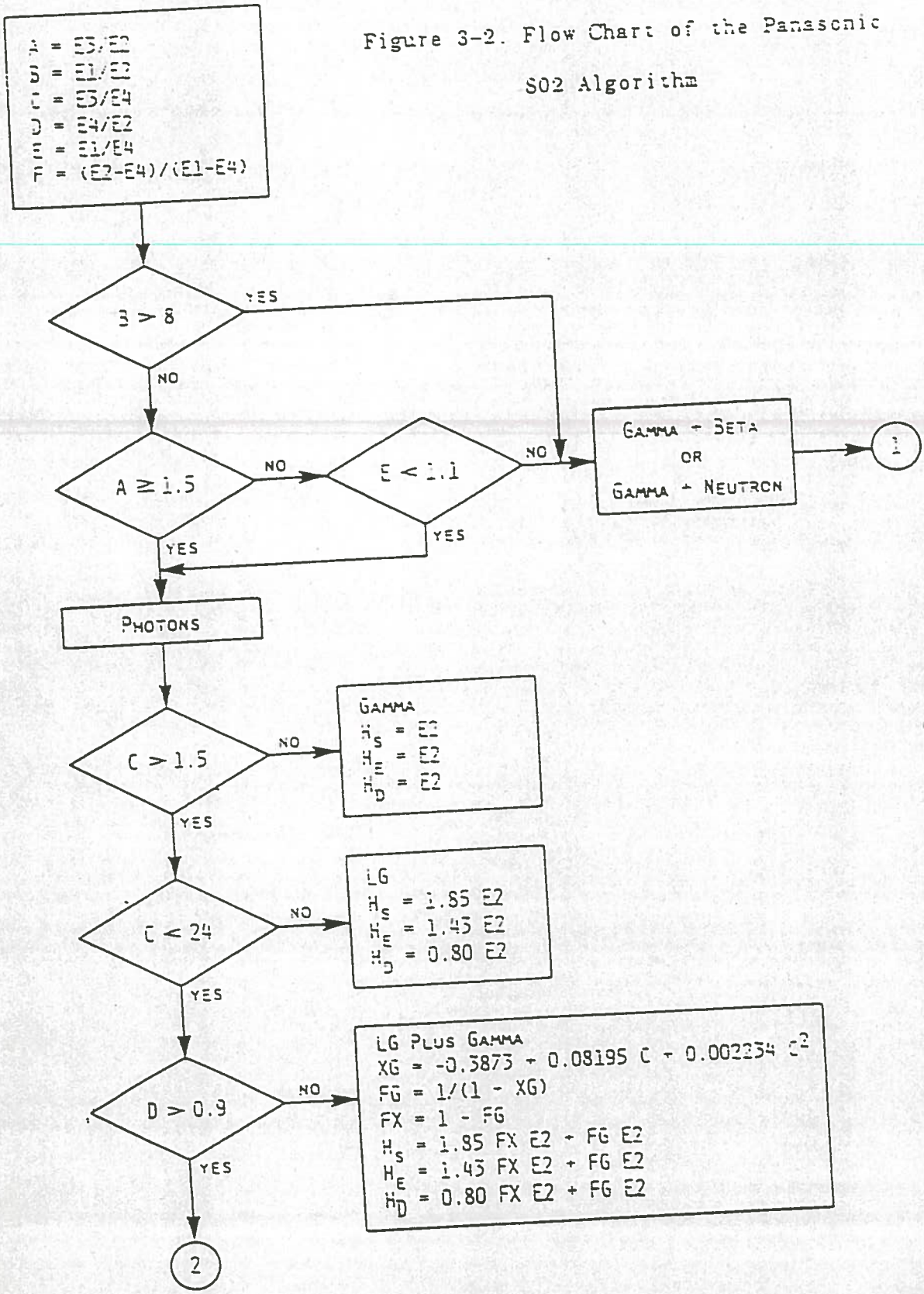

Figure 3-2. Flow Chart of the Panasonic S02 Algorithm

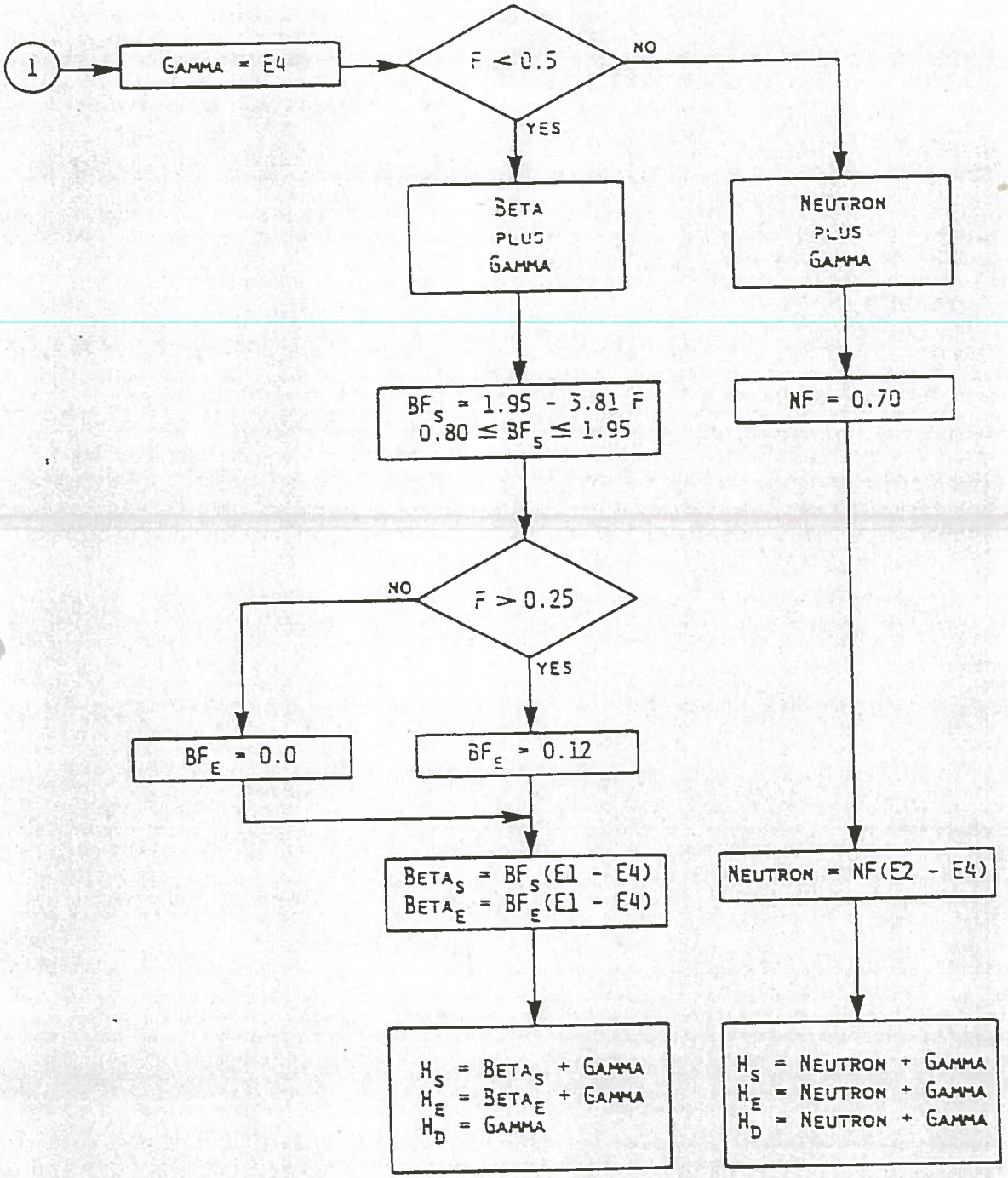

Figure 3-2. Flow Chart of the Panasonic 802 Algorithm

(continued)

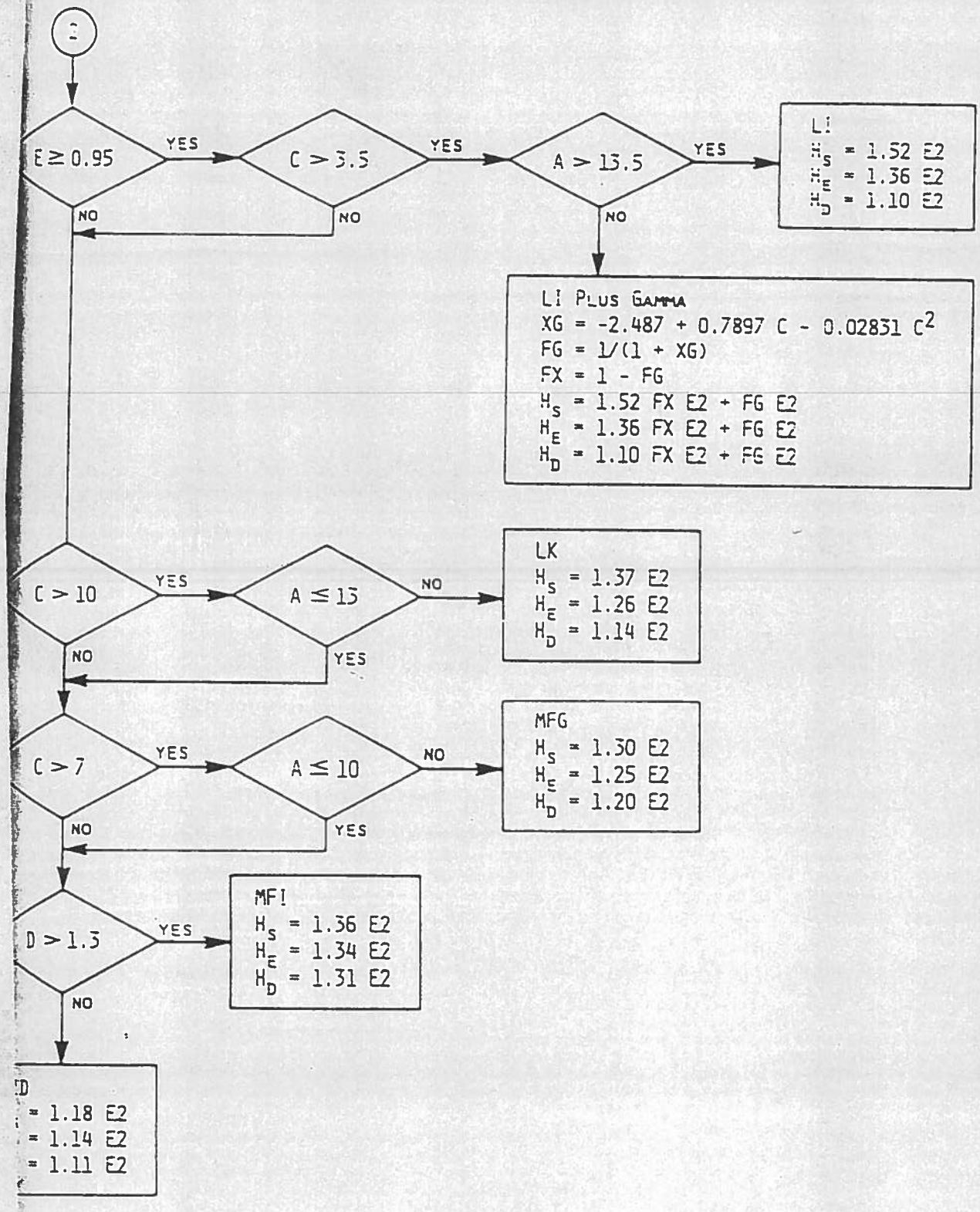

Figure 3-2. Flow Chart of the Panasonic 802 Algorithm

(continued)

To determine neutron dose for the particular packets used the following formula is used:

$$H_D(\text{mrem}) = NF * (E2-E4)$$

where:

H_D= reported neutron dose equivalent

NF = neutron factor (mrem/mR*)

E2 = response of element 2 (mR*)

E4 = response of element 4 (mR*)

For the NVLAP approved TLD irradiation source, a 30 cm dia. sphere of D_2O moderated ^{252}Cf is used. The spectra from this source yields a NF of 0.7. It was believed that this spectra most closely resembles the spectra found in commercial nuclear power plants. This NF (0.70)is appropriate for the californium spectrum only and for each different spectrum a new NF must be generated.

Waterford, in order to determine plant specific NFs, has conducted several studies with Panasonic 802 TLDs (P183). In the first study, Waterford's TLDs were exposed to three different neutron sources. These were: an unmoderated PuBe source, a D_2O moderated ^{252}Cf source , and the J-port of a research reactor (the J-port is a column leading off the reactor that allows only thermal neutrons to exit). This study demonstrates the response dependence of NFs as a function of the thermal neutrons present. The PuBe source is a very hard spectrum with an average energy of approximately 4.5 MeV. In this neutron spectrum the

Panasonic 802 underresponds by a factor of twelve. The Panasonic 802 exposed to the more thermalized spectra of the moderated californium overresponds by a factor of 1.22. The Panasonic 802 exposed to the J-Port, which has an average energy of approximately 0.051 eV, had a very high response to these neutrons. The response was fourteen times the actual dose.

In light of this study, Waterford requested a study of neutron dose rates inside of containment to determine appropriate NFs (So85). From this study location specific NFs were generated in Waterford's containment at locations outside the D-rings. Utilizing this study and containment blueprints, a correlation between NFs and concrete thickness between the reactor vessel and measurement location was determined. This is accomplished by dividing a TEPC measurement (mrem) by the response of a TLD in the same location. For example, to determine the NF associated with 8 ft of concrete, the +46 ft. level laydown area (Fig. 1-3) provides approximately 8 ft of concrete between the measurement location and the reactor vessel, therefore:

$$NF = \frac{\text{TEPC measurement (mrem)}}{\text{neutron response mR*}}$$

$$= \frac{388.5 \text{ mrem}}{2807.1 \text{ mR*}}$$

$$= 0.138$$

The NFs determined for different thicknesses are listed in Table 3-4. This relationship exists as a result of the moderation provided by the concrete - the more concrete, the more thermalized the spectrum and the more the TLD responds. From this correlation the minimum NF (i.e. largest response correction) for the 802 TLD inside containment at Waterford was 0.0219.

As part of its quality control program, Waterford has participated in the ninth, tenth, and twelth Personnel Dosimetry Intercomparison Study (PDIS) at Oak Ridge National Laboratory. The PDIS utilizes the Health Physics Research Reactor (HPRR), part of the Dosimetry Applications Research Facility, to perform research in health physics and biomedical fields. The HPRR is a small, unshielded and unmoderated reactor using highly enriched ^{235}U, alloyed with ten percent molybdenum by weight, as the fuel material. The fuel is a cylindrical rod nine inches high and eight inches in diameter.

Waterford presented three TLD badges (UD-802) for six different shielding exposures. One of these exposures included a ^{137}Cs source combined with the HPRR for a gamma interference. Another exposure consisted of a PuBe source only, while the remaining exposures were with the HPRR only. Refer to Table 3-4 for the shielding moderators for the HPRR only runs.

The phantoms used for the exposures were 40 by 40 by 15 cm lucite blocks. The phantoms were located three meters and four meters from the HPRR. Reference neutron dosimetry for the HPRR is developed from spectral measurements for the unshielded reactor with lucite, concrete,

Table 3-3. Neutron Factors as a Function of Concrete Thickness Between Reactor vessel and Measurement Location

Elevation Inside Containment (ft)	Thickness of Concrete (ft)	Neutron Factor
-4	25	0.0219
-4	20	0.0305
+21	14	0.0636
-4	13	0.0769
+21	13	0.0771
+21	12	0.0875
+21	12	0.1045
+21	10	0.1045
+21	10	0.1094
+21	10	0.1147
+46	8	0.1373
+46	8	0.1400

and steel moderators as well as combinations of each.

From these exposures TLD correction factors were generated for both moderated and nonmoderated neutron spectra. These studies also demonstrated the thermal dependence of the neutron response of the Panasonic 802s. The most recent study in which Waterford participated generated the NFs contained in Table 3-4.

Arkansas Nuclear One - Unit 2 (ANO) is a Combustion Engineering (CE) PWR similar in design to Waterford. Using neutron activation techniques and spectral unfolding the neutron energy spectrum in both the reactor core and reactor pressure vessel cavity have been determined (Ts85). The neutron spectra from the core midplane elevation outside the pressure vessel is graphed in Figure 3-3. Plotted with this is a spectrum produced from the HPRR with concrete, steel, and lucite moderation (Si87). When overlaid, the spectra appear very similar. The reason for this similarity is due to the similar attenuating materials used by the HPRR. As a result of the similarity of these spectra a TLDs response to both should be similar. This assumption means that the maximum NF to be found in the containment of a CE pressurized water reactor is that NF generated by the moderated HPRR, or 0.32. Since all other areas inside containment at Waterford will have a more thermalized spectra than the core or cavity a NF below 0.32 is appropriate. Therefore the upper and lower limits of NFs inside containment at Waterford have been assumed. The upper limit is assumed to be 0.32, and the lower limit 0.0219.

Table 3-4. TLD Calibration Factors Generated in the Twelth Personnel Dosimetry Intercomparison for the Panasonic 802

Reactor Moderation Format	NF
Bare PuBe source	4.69
HPRR unshielded	1.74
HPRR shielded by boron and Steel	1.42
HPRR shielded by 20 cm concrete	0.72*
HPRR shielded by 15 cm concrete, 5 cm steel	0.68*
HPRR shielded by lucite	0.31
HPRR shielded by steel, concrete, and lucite	0.32
HPRR shielded by lucite and gamma enhanced	0.23

* From 9th and 10th PDIS and Corrected for New HPRR Configuration

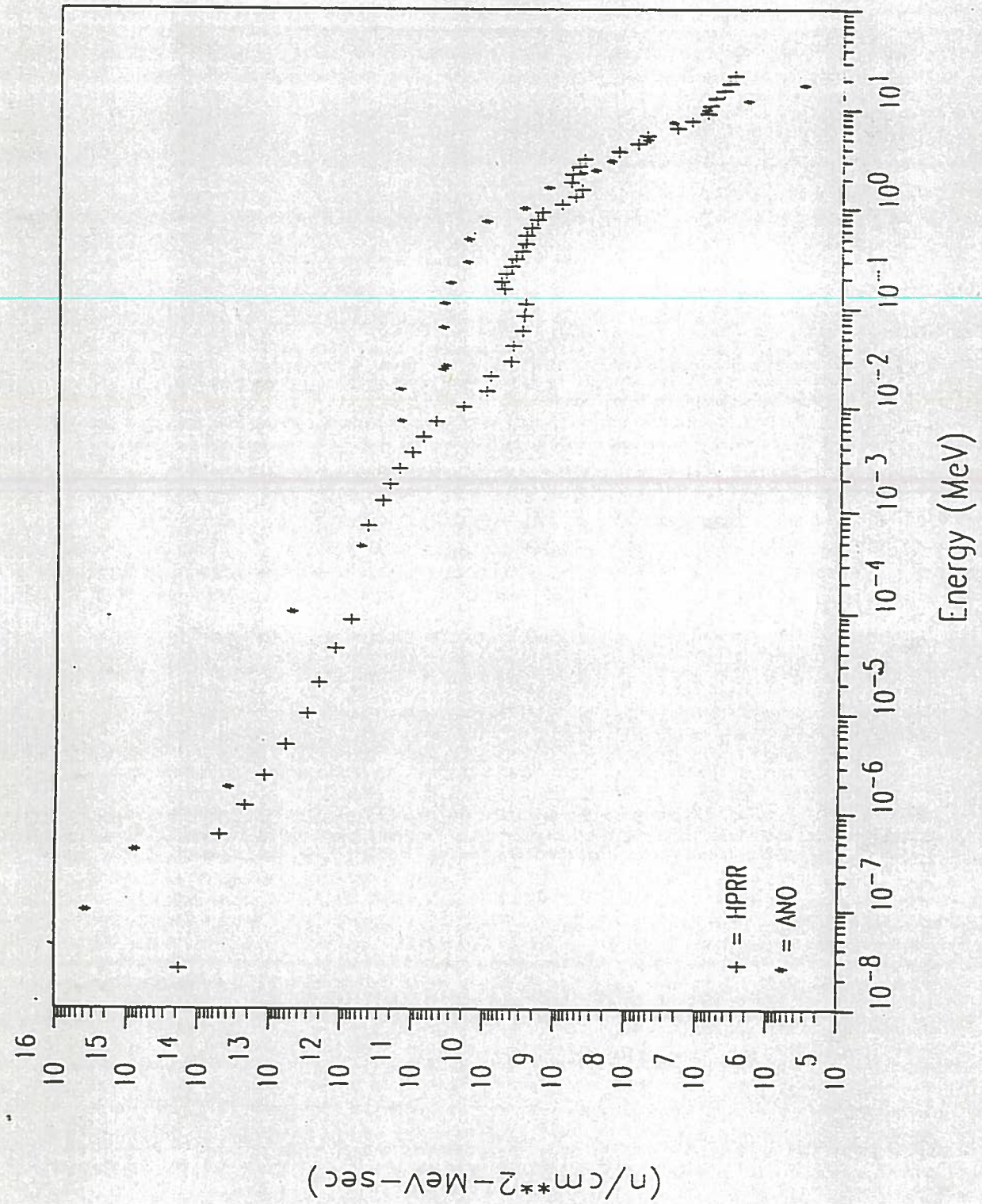

Figure 3-3. HPRR with Concrete, Steel, and Lucite Moderator Compared to ANO-2 Core Midplane Inside the Pressure Vessel Cavity

3.5 Fluence to Dose Conversion

It is important to note that there are many conventions for fluence to dose conversion factors (NCRP38, ICRP21, Au68, Ch81, NRC). Table 3-5 lists the conventions currently in practice. Significant variations in conversion factors exist for all five conventions, however the overall difference between methods is less than 20%. Although the total variation is small, some dose conversion factors vary considerably between conventions. For example at 0.1 MeV the variation between the Auxier (Au68) and the NRC (NRC) methods is 71% and for 0.5 MeV the difference between the NCRP 38 and Auxier (Au68) methods is 36%. Probable causes for the variations include the type of phantom used, the percent composition of elements for the "standard man", the Monte Carlo computer code used, and the cross section library. Because conversion factors can vary from convention to convention, it is necessary that a consistant method be utilized for determination of dose equivalent. All methods used to determine NFs at Waterford have utilized the method proposed by ICRP Report No. 21 (ICRP21).

3.6 Calculation of Thermal and Resonance Flux

Determination of neutron flux by radioactivation techniques is performed using the American Standard for Testing and Materials (ASTM77) method because of high tempertures, foil self shielding, and foil geometry. This method describes the general procedure for determining an unknown neutron flux by neutron activation.

Most neutron fluence rates are made in a field of neutrons where all neutron energies are present, not just thermal neutrons. Therefore

Table 3-5 Neutron Fluence to Dose Conversion Factors from Five Different Conventions (DE/Fluence, 10^{-5} mrem-cm^2)

E, MeV	NCRP	ICRP	NRC	Auxier	Chilton
thermal	0.102	0.107	0.103	0.115	0.095
1E-7	0.102	0.116	-	-	-
1E-6	0.124	0.126	-	0.134	0.118
1E-5	0.124	0.121	-	0.121	0.116
1E-4	0.120	0.116	0.139	0.101	0.110
1E-3	0.102	0.103	-	0.086	0.095
5E-3	-	-	0.122	-	-
1E-2	0.099	0.099	-	0.099	0.095
2E-2	-	-	0.025	-	-
0.1	0.604	0.579	0.833	0.486	0.781
0.5	2.57	1.98	2.33	1.89	2.44
1	3.65	3.27	3.85	3.26	3.79
2	-	3.97	-	-	-
2.5	3.47	-	3.45	3.50	3.41
5	4.34	4.08	3.85	4.41	3.90
7	4.08	-	-	4.03	-
7.5	-	-	4.17	-	4.11
10	4.08	4.08	4.17	4.31	4.14
14	5.79	-	-	6.15	5.26

determination of thermal and epithermal flux is performed by irradiation of activation foils. The foils used in this study were bare gold foils for determination of thermal and epithermal fluxes and cadmium covered gold and indium for resonance fluxes. Since activation of a bare gold foil is a measurement of both thermal and epithermal neutrons, determination of the amount of activation due to epicadmium neutrons on a foil is required. This is accomplished by encapsulating a gold foil inside a cadmium cover. For a thicknesses of 0.04 in. cadmium essentially absorbs all neutrons having energies less than about 0.5 eV, thus eliminating thermal neutron activation. By extracting the activity of epicadmium neutrons from the bare gold foil a measurement of thermal neutrons is determined.

The saturation activity of a bare gold or indium foil irradiated in a mixed neutron field is given by:

$$A_s = \phi_{th} * g * \sigma_0 + \phi_e * g * \sigma_0 (f_1 + w'/g + I_0/g\sigma_0) \qquad (1)$$

where

ϕ = total thermal neutron flux

g = correction factor for departures from the 1/v detector cross section for thermal neutrons

σ_0 = 2200 m/s cross section

ϕ_e = epithermal neutron flux

f_1 = function that describes the epithermal activation of a

of a 1/v detector in the energy range of 5kT to E_{cd}

where E_{cd} is cadmium's resonance cross section

maximum energy

w' = function which accounts for departure of the cross section from the 1/v law in the energy range of 5kT to E_{cd}

I_o = resonance integral cross section for an ideal dilute detector

For a cadmium covered gold or indium foil the saturation activity is given as:

$$A_{s,cd} = \phi_e * I_o \qquad (2)$$

Equation (2) can be used to eliminate the epithermal flux parameter, ϕ_e, from equation (1). After rearrangement, one obtains an expression for the saturation activity due to thermal neutrons:

$$(A_s)_{th} = A_s - A_{s,cd} [\, 1 + (g\sigma_o/G_{res})f_1 + (\sigma_o w'/G_{res} I_0)] \qquad (3)$$

where

G_{res} = value for self shielding factor of foil thickness

Therefore when a bare gold foil has been activated by neutrons, the

following relationship is true:

$$\phi_{th} = K * (A_s)_{th} \qquad (4)$$

where K is a constant for any given size foil and counting set up. The constant K includes the counter efficiency, the macroscopic nuclear properties of the foil, and the geometry of the foil and detector.

Determination of the epithermal saturation activity can now be calculated by equation (3). Assuming thermal neutrons do not reach the activation foil, $(A_s)_{th}$ equals zero and solving for $A_{s,cd}$ reveals the epithermal saturation activity. This activity can then be incorporated into equation (2) for resonance flux. Note that for a bare foil in a mixed neutron spectrum, the cadmium covered gold foil resonance saturation activity must first be determined to solve for thermal saturation activity. Once thermal saturation activity has been determined equation (4) is used for calculation of thermal flux.

Determination of the resonance flux for a cadmium covered indium foil follows the same method as that used to calculate the resonance flux for cadmium covered gold (Eqs. 2,3). Parameters used in equations 1-4 can be found in tables listed in (ASTM77). It is noted that the resonance fluxes determined are integral fluxes and are used for spectral estimation only. More details on techniques for determining neutron thermal and resonance fluxes by radioactivation techniques may be found in the references (Be64, Ts81).

3.7 Neutron Energy Spectra Inside and Outside the D-Rings

The neutron energy spectra generated in Figures 3-4 and 3-5 are based on neutron activation, instrumental surveys from previous studies using TEPC and ^{3}He spectrometers, and postulation from the characteristics of spectra from other reactors (ANO, HPRR).

The spectrum for the refueling cavity was estimated by neutron activation results, postulated similarity to the HPRR and ANO spectra, and TEPC measurements previously taken inside containment (So85). In the thermal region and part of the intermediate region, fluences were estimated by activation results. Because of large resonance cross sections of the gold and indium activation samples for thermal, 1.457 eV, and 4.906 eV energies, it is assumed that most of the activation for these resonances are a result of neutron energies within the resonances. The thermal flux was determined using ASTM methods. These methods were also used at the resonance energies of 1.457 eV, and 4.906 eV (Sec. 3.6). Plotting these determined fluxes as a function of the neutron energies produces the low energy component of the spectrum. In addition to the thermal component, an estimate of the average neutron flux above a threshold energy of 1.2 MeV was determined. This integral flux estimate provides an upper boundary for the fast neutron component. It is stressed that the determined fluxes are not discrete fluxes and are used only for spectral estimation. By using the characteristics of the 26 group ANO and 56 group HPRR spectra, the rest of the spectrum was postulated.

The spectrum for the S/G hotleg was estimated using the same approach as the refueling cavity. By neutron activation, the thermal

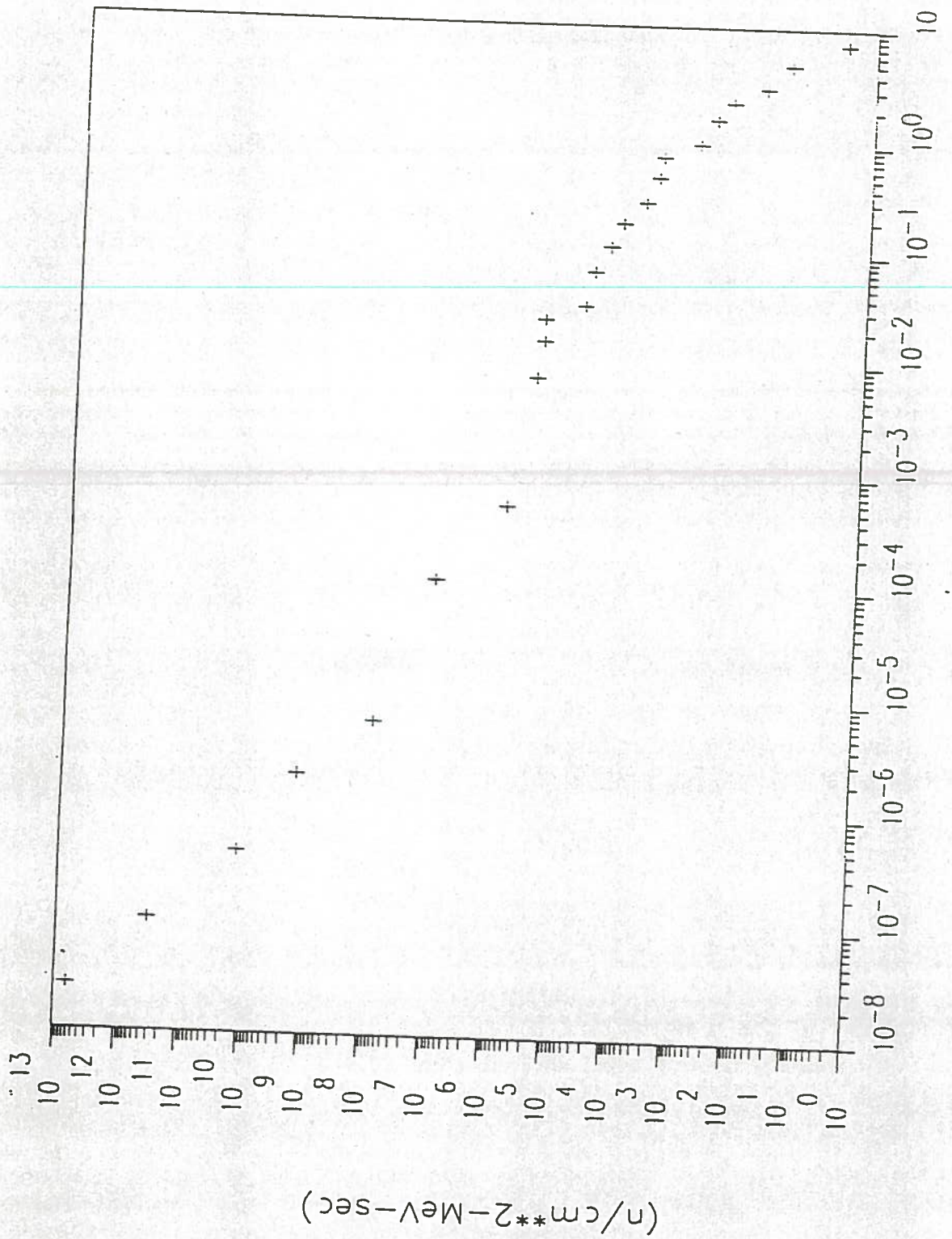

Figure 3-4. Estimated Neutron Energy Spectra for the Steam Generator Hotleg

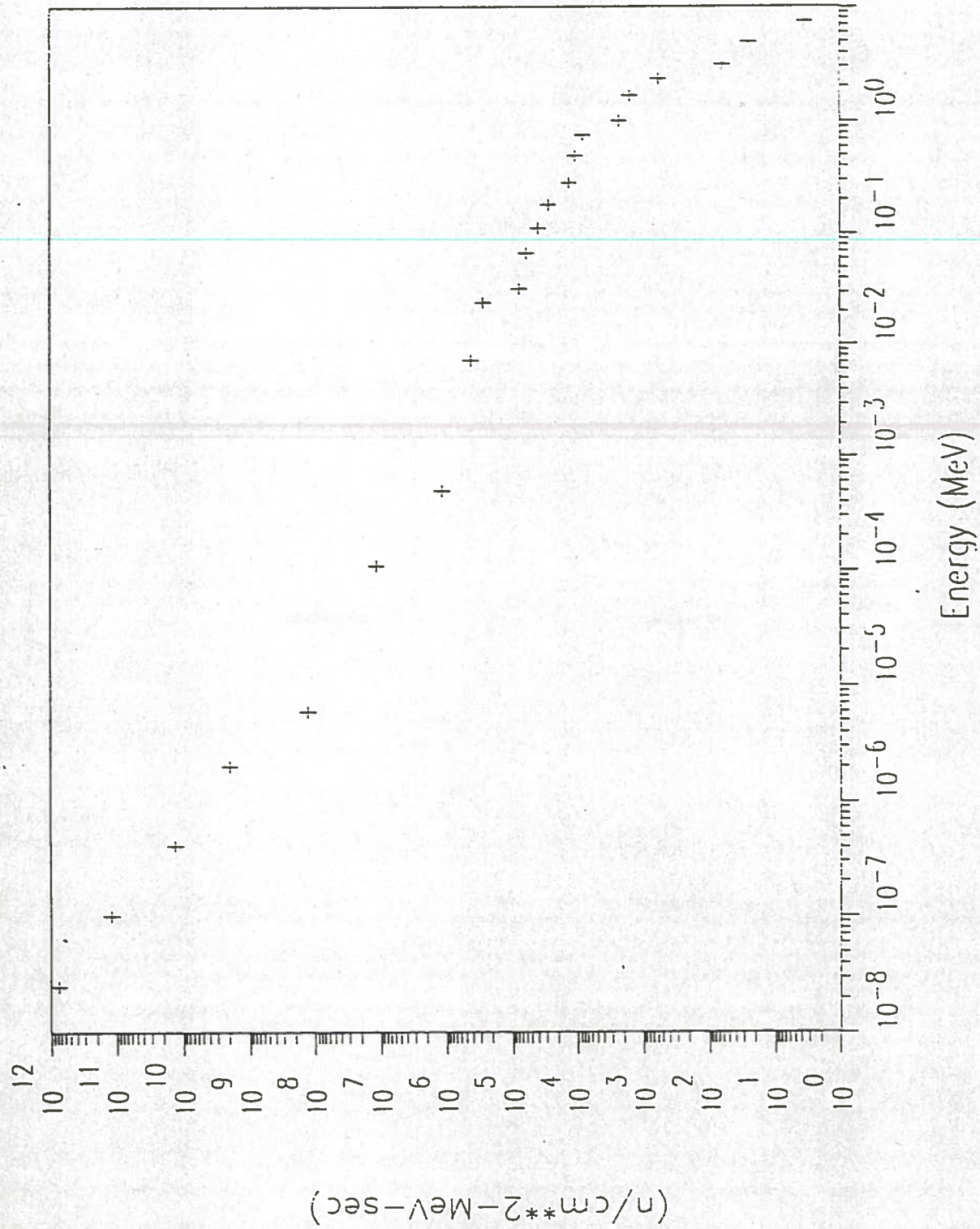

Figure 3-5. Estimated Neutron Energy Spectra for the Refueling Cavity

component and part of the intermediate neutron component was determined. The energy range from 4.906 eV to 10 KeV was postulated by the characteristics of the HPRR and ANO spectra. The activation packet at the #2 S/G hotleg demonstrated the lack of sufficient high energy neutrons above 1.2 MeV threshold for activation. Therefore it was assumed that the neutron fluence in the fast region falls below that of the refueling cavity. Counting statistics obtained from the gamma spectroscopy analysis of the indium activation foil were used to determine a minimum detectable reaction rate. Assuming that this activity induced was present but not measured, a minimum detectable flux above a 1.2 MeV threshold associated with this activity is approximately 1.5E+3 neutrons per centimeter squared per second. Since this is the threshold integral flux, the remainder of the neutron spectra for the S/G hotleg can be postulated referring to the previous spectra generated for the refueling cavity and bounding the total to 1.5E+3 neutrons per centimeter per squared second. It appears that the penetrations through the primary shield into the D-rings allow thermal neutrons to transmit from the reactor pressure vessel cavity into the D-rings. This would explain the large thermal tail for the S/G hotleg spectra.

The neutron spectrum for the #1 S/G platform, and #2 S/G platform, and #1 S/G hotleg are assumed to have a neutron spectrum similar to that of the #2 S/G hotleg since they are within the primary shield streaming paths. The neutron spectrum for the #1B RCP ladder and the #2B ladder and RCP strainers are assumed to more thermalized and lower in flux than the S/G hotleg because the amount of concrete present between these locations and the RV and the fact that streaming paths contributions are

minimal.

In order to determine the accuracy of the estimated spectra for the refueling cavity and the S/G hotleg, the differential energy spectra shown in Figure 3-4 was transformed into a multigroup flux spectra. The spectrum was transformed into 56 groups for the most accurate estimate. From this multigroup spectra and the fluence to dose conversion factors of ICRP 21, the neutron dose equivalent rate for the refueling cavity can be determined. By multiplying the multigroup flux by its appropriate fluence to dose conversion factor, a dose rate was calculated for each particular group. Flux to dose conversion factors for energy groups not equal to those listed by ICRP 21 were determined by interpolation. The total dose rate is a summation of the dose rates for each group. Table 3-6 lists the energy group, flux, fluence to dose conversions, and dose rates.

The dose rate calculated from the estimated spectra for the refueling cavity is 5.8 rem/hr. A TEPC measurement in approximately the same location as the activation packet resulted in a dose rate of 4.8 rem/hr (So85). Comparing these two dose rates it is apparent that the estimated spectra overestimates the dose. This inaccuracy is most probably due to the "rough" method of piecing together a spectra. But in retrospect is appears that this spectra is a good approximation of the general shape of the true spectra.

Table 3-6. Transformation of Estimated Neutron Energy Spectrum for the Refueling Cavity Into a Dose Rate Using ICRP 21

Group	Flux (n/cm^2-sec)	Conversion (mrem-cm^2)	Dose Rate (mrem/sec)
1	5.62E+4	1.07E-6	6.01E-2
2	1.99E+4	1.23E-6	2.45E-2
3	1.68E+4	1.26E-6	2.12E-2
4	1.47E+4	1.26E-6	1.85E-2
5	1.26E+4	1.25E-6	1.58E-2
6	1.17E+4	1.24E-6	1.45E-2
7	1.09E+4	1.22E-6	1.33E-2
8	1.03E+4	1.19E-6	1.23E-2
9	1.37E+4	1.16E-6	1.59E-2
10	1.59E+4	1.13E-6	1.80E-2
11	1.68E+4	1.09E-6	1.83E-2
12	1.57E+4	1.05E-6	1.65E-2
13	1.11E+4	1.03E-6	1.14E-2
14	1.17E+4	1.02E-6	1.19E-2
15	1.12E+4	1.01E-6	1.13E-2
16	8.42E+3	1.01E-6	8.54E-3
17	4.61E+3	1.00E-6	4.61E-3
18	3.82E+3	9.97E-7	3.81E-3
19	3.52E+3	9.91E-7	3.49E-3
20	3.57E+3	1.31E-6	4.68E-3
21	4.58E+3	1.71E-6	7.83E-3
22	5.59E+3	2.24E-6	1.25E-2
23	8.32E+3	2.94E-6	2.44E-2
24	9.99E+3	3.87E-6	3.87E-2
25	1.58E+3	5.05E-6	7.98E-3
26	1.83E+3	6.24E-6	1.14E-3
27	1.21E+3	7.08E-6	8.57E-3
28	2.26E+3	8.14E-6	1.84E-3
29	2.31E+3	9.32E-6	2.15E-3
30	2.37E+3	1.07E-5	2.54E-2
31	2.42E+3	1.22E-5	2.95E-2
32	2.58E+3	1.40E-5	3.61E-2
33	2.60E+3	1.60E-5	4.16E-2
34	3.08E+3	1.83E-5	5.64E-2
35	3.39E+3	2.10E-5	7.12E-2
36	3.40E+3	2.37E-5	8.06E-2
37	3.38E+3	2.71E-5	9.16E-2
38	3.19E+3	3.08E-5	9.83E-2
39	2.81E+3	3.35E-5	9.41E-2
40	2.82E+3	3.52E-5	9.93E-2

Table 3-6. Transformation of Estimated Neutron Energy Spectrum for the Refueling Cavity Into a Dose Rate Using ICRP 21

Group	Flux (n/cm^2-sec)	Conversion (mrem-cm^2)	Dose Rate (mrem/sec)
41	2.99E+3	3.71E-5	1.11E-2
42	1.78E+3	3.90E-5	6.94E-2
43	1.23E+3	3.98E-5	4.90E-2
44	8.62E+2	4.00E-5	3.45E-3
45	8.50E+2	4.03E-5	3.43E-3
46	8.61E+2	4.05E-5	3.49E-3
47	8.70E+2	4.08E-5	3.55E-3
48	8.45E+2	4.08E-5	3.45E-3
49	7.61E+2	4.08E-5	3.11E-3
50	6.51E+2	4.08E-5	2.66E-3
51	2.78E+2	4.08E-5	1.13E-3
52	2.61E+1	4.11E-5	1.07E-4
52	1.03E+0	4.15E-5	4.27E-5
53	-	-	-
54	-	-	-
55	-	-	-
56	-	-	-
			1.609

Total Dose Rate = 1.609 mrem/sec * 3600 sec/hr = 5.8 rem/hr

TEPC measurement in same location = 4.8 rem/hr

Chapter Four

RESULTS, CONCLUSIONS, and RECOMMENDATIONS

4.1 QAD-CG Results

Because QAD calculations are divided into three different sources, the reactor vessel, S/G hotleg plenum, and the S/G tubing, the results are a combination of each source. Initially it was expected that the reactor vessel would contribute the majority of the gamma dose rates inside the D-rings. However the S/G was clearly the main source of gamma radiation. Tables 4-1 through 4-6 list the dose rates according to the energy group, average energy of each group, and the gamma energy flux.

The dose rates at each RCP ladder are similar, 2.75 R/hr and 3.5 R/hr. The dose rates nearest the S/G are much higher, 7.2 R/hr at the hotleg and 9.2 R/hr at the platform. The dose rates at the RCP strainers are considerably lower than all other locations calculated due to shielding provided by the RCPs since the strainer is located behind the RCP.

Even though the gamma radiation emanating from the reactor vessel is significant, the primary shield wall provides enough attenuation to significantly decrease the gamma flux within the D-rings. Locations where the reactor vessel contributes to the gamma dose rate are the S/G hotleg and the RCP ladders. The penetrations through the primary shield into the D-rings provide a streaming path that create an elevated gamma flux in these particular locations, however this flux is still quite low when compared to the flux produced by the S/G. All other locations

Table 4-1. Gamma Dose Rates at Reactor Coolant Pump 2A Ladder Calculated by QAD-CG

Energy Group (MeV)	Group Avg. Energy (MeV)	Energy Flux (MeV/cm^2-s)	Dose Rate* (mR/hr)
0.01 - 0.25	0.044	4.632E+2	9.971E+0
0.25 - 0.60	0.284	6.484E+2	7.876E+0
0.60 - 0.80	0.679	1.835E+3	1.449E+1
0.80 - 1.25	1.215	4.221E+3	2.256E+1
1.25 - 1.75	1.500	1.185E+3	1.890E+1
1.75 - 3.00	2.303	5.036E+3	3.174E+1
3.00 - 4.00	3.500	5.266E+3	2.833E+1
4.00 - 5.00	4.500	7.570E+3	3.110E+1
5.00 - 6.00	5.500	9.278E+3	3.242E+1
6.00 - 7.00	6.129	2.005E+6	3.227E+3
7.00 - 8.00	7.500	1.307E+4	3.505E+1
8.00 - 9.00	8.500	8.333E+3	1.913E+1
9.00 - 10.0	9.500	1.110E+3	2.223E+0
Total:		2.063E+6	3.481E+3

*All dose rates include buildup

Table 4-2. Gamma Dose Rates at the #2 Steam Generator Hotleg Calculated by QAD-CG

Energy Group (MeV)	Group Avg. Energy (MeV)	Energy Flux (MeV/cm^2-s)	Dose Rate* (mR/hr)
0.01 - 0.25	0.044	1.281E+3	2.549E+1
0.25 - 0.60	0.284	1.572E+3	1.604E+1
0.60 - 0.80	0.679	3.844E+3	2.531E+1
0.80 - 1.25	1.215	8.776E+3	4.042E+1
1.25 - 1.75	1.500	1.334E+1	5.702E-1
1.75 - 3.00	2.303	4.117E+3	1.634E+1
3.00 - 4.00	3.500	1.074E+3	1.052E+1
4.00 - 5.00	4.500	2.771E+3	1.866E+1
5.00 - 6.00	5.500	4.890E+3	2.602E+1
6.00 - 7.00	6.129	4.352E+6	6.963E+3
7.00 - 8.00	7.500	1.035E+4	3.850E+1
8.00 - 9.00	8.500	7.576E+3	2.334E+1
9.00 - 10.0	9.500	1.117E+3	2.928E+0
Total:		4.400E+6	7.719E+3

*All dose rates include buildup

Table 4-3. Gamma Dose Rates at the #2 Steam Generator Platform Calculated by QAD-CG

Energy Group (MeV)	Group Avg. Energy (MeV)	Energy Flux (MeV/cm^2-s)	Dose Rate* (mR/hr)
0.01 - 0.25	0.044	1.682E+3	3.543E+1
0.25 - 0.60	0.284	2.167E+3	2.193E+1
0.60 - 0.80	0.679	5.184E+3	3.360E+1
0.80 - 1.25	1.215	1.134E+4	5.099E+1
1.75 - 3.00	2.303	4.958E+3	1.558E+1
6.00 - 7.00	6.129	5.708E+6	9.642E+3
Total:		5.733E+6	9.200E+3

*All dose rates include buildup

Table 4-4. Gamma Dose Rates at Reactor Coolant Pump 2B Ladder Calculated by QAD-CG

Energy Group (MeV)	Group Avg. Energy (MeV)	Energy Flux (MeV/cm^2-s)	Dose Rate* (mR/hr)
0.01 - 0.25	0.044	5.198E+1	5.339E+0
0.25 - 0.60	0.284	3.186E+2	1.032E+1
0.60 - 0.80	0.679	9.392E+2	1.257E+1
0.80 - 1.25	1.215	2.318E+3	8.420E+0
1.25 - 1.75	1.500	4.466E+3	5.667E+1
1.75 - 3.00	2.303	9.321E+3	6.218E+1
3.00 - 4.00	3.500	1.254E+4	5.780E+1
4.00 - 5.00	4.500	1.617E+4	5.809E+1
5.00 - 6.00	5.500	1.842E+4	5.713E+1
6.00 - 7.00	6.129	1.183E+6	2.333E+3
7.00 - 8.00	7.500	2.374E+4	5.765E+1
8.00 - 9.00	8.500	1.467E+4	3.073E+1
9.00 - 10.0	9.500	1.913E+3	3.509E+0
Total:		1.288E+6	2.753E+3

*All dose rates include buildup

Table 4-5. Gamma Dose Rates at Reactor Coolant Pump 2A Strainer Calculated by QAD-CG

Energy Group (MeV)	Group Avg. Energy (MeV)	Energy Flux (MeV/cm^2-s)	Dose Rate* (mR/hr)
0.01 - 0.25	0.044	4.175E+1	1.214E+0
0.25 - 0.60	0.284	9.004E+1	1.087E+0
0.60 - 0.80	0.679	5.085E+2	4.568E+0
0.80 - 1.25	1.215	1.229E+3	6.699E+0
1.75 - 3.00	2.303	7.004E+2	2.494E+0
6.00 - 7.00	6.129	4.957E+5	8.054E+2
Total:		4.983E+5	8.214E+2

*All dose rates include buildup

Table 4-6. Gamma Dose Rates at Reactor Coolant Pump 2B Strainer Calculated by QAD-CG

Energy Group (MeV)	Group Avg. Energy (MeV)	Energy Flux (MeV/cm^2-s)	Dose Rate* (mR/hr)
0.01 - 0.25	0.044	4.142E+1	1.098E+0
0.25 - 0.60	0.284	9.145E+1	1.068E+0
0.60 - 0.80	0.679	5.544E+2	4.903E+0
0.80 - 1.25	1.215	1.318E+3	7.065E+0
1.75 - 3.00	2.303	7.451E+2	2.617E+0
6.00 - 7.00	6.129	5.045E+5	8.146E+2
Total:		5.072E+5	8.313E+2

*All dose rates include buildup

inside the D-rings with the reactor vessel source produced an insignificant gamma flux. For this reason the dose rates at the RCP strainers and S/G platforms include those energy groups produced by the S/G only.

Referring to Tables 2-2 and 2-3, ^{16}N is the nuclide with both the highest activity and highest gamma energy per disentegration in the reactor coolant. Because of its high specific activity and its high gamma energy, ^{16}N produces most of the gamma dose present in the D-rings at full power. The production of ^{16}N in the reactor coolant is a result of fast neutron activation of ^{16}O. Within a short period of time after reactor shutdown ^{16}N activity is nonexistant due to its short halflife (i.e. 7.1 seconds). Therefore the gamma dose rates inside the D-rings will decrease considerably with time after shutdown.

In the study by Clark (Cl87) the gamma dose rate at the -4 ft. bioshield void was reported as 10 mR/hr. A detector located at approximately the same location in the QAD-CG model calculated a dose rate of 4.5 mR/hr. This dose rate is less than half that determined by Clark. It is assumed that the reason for this discrepancy is that not all sources were included in the model. The major sources of gamma radiation inside the D-rings are included, but these are not the only sources. Other sources include capture gammas produced by leakage neutrons, the reactor coolant system piping, and the RCP's. The latter two sources contain reactor coolant at the same specific activity of ^{16}N as the S/G.

4.2 Site Specific Neutron Factors Inside the D-Rings

It was determined that the NFs inside the D-rings ranged between 0.14 and 0.022. These NFs were determined from the correlation of concrete thickness moderating the neutron spectra. In Table 3-3, it was seen that the highest measured TLD overresponse occured in an area with 25 ft. of concrete between the RV and the measurement location. This thickness corresponds to the NF of 0.022. In areas with the minumum amount of concrete shielding (i.e. 8 ft.) the TLD overresponded by seven times for a NF of 0.14. Since approximately 8 ft. of concrete is between the RV and the inside of the D-rings at the RCP strainers, it was estimated that the NFs inside the D-rings should be 0.14 for these locations outside of piping streaming paths. For those areas inside the D-rings near piping penetrations, the highly thermalized S/G hotleg spectrum would generate a NF between 0.14 and 0.022. As a result of these assumptions and spectral evaluations, the NFs for TLDs located in streaming paths were assigned a NF of 0.09. Thermoluminescent dosimeters located outside streaming paths on the ladders to the S/G platform were assigned a NF of 0.14 which is consistent with concrete shielding between their location and the RV.

Since the Panasonic 802 responds more to thermal neutrons compared high energy neutrons, the area inside containment at Waterford producing the least response on a Panasonic 802 TLD would be that area with the hardest spectrum. Of all locations inside containment the reactor cavity was determined to have the hardest spectrum because of the high fluence of fast neutrons detected. At this location, the appropriate NF is that determined by intercomparison with the HPRR, 0.32.

Figure 4-1 illustrates the location of different NFs and their assigned values.

4.3 TLD Results

Analyses of the TLD response inside the D-rings and reactor cavity are presented in Table 4-7. The results of QAD-CG and previous studies (Cl87,Es88) were used to extract the gamma dose rates for determination of the neutron response and dose equivalent. Each activation packet contained two TLDs so the averaged response of each pair of TLDs were used in the analysis. The gamma dose rate was subtracted from the average TLD response (Avg.mR*) and multiplied by the NFs generated inside the D-rings to result in the neutron dose equivalent for each location surveyed. Because of the uncertainty of the NFs used in the previous study inside the D-rings (Es88) those locations surveyed and the reponse of the TLDs are incorporated into this study.

As expected, the dose rates for the reactor cavity and the S/G hotleg are significantly high, 4.8 rem/hr and 3.1 rem/hr respectively. The neutron dose rate at the S/G hotleg is high as a result of the penetration through the primary shield. This penetration allows the leakage neutrons from the reactor vessel cavity to migrate into the D-rings at a much higher flux than areas outside this streaming path. As a result the neutron dose rate is higher than any other location within the D-rings. The neutron dose rate in the reactor cavity is high due to the fact that there is a higher energy neutron fluence due to less concrete shielding. This high fluence was identified by neutron activation and previous instrumental measurements (So85).

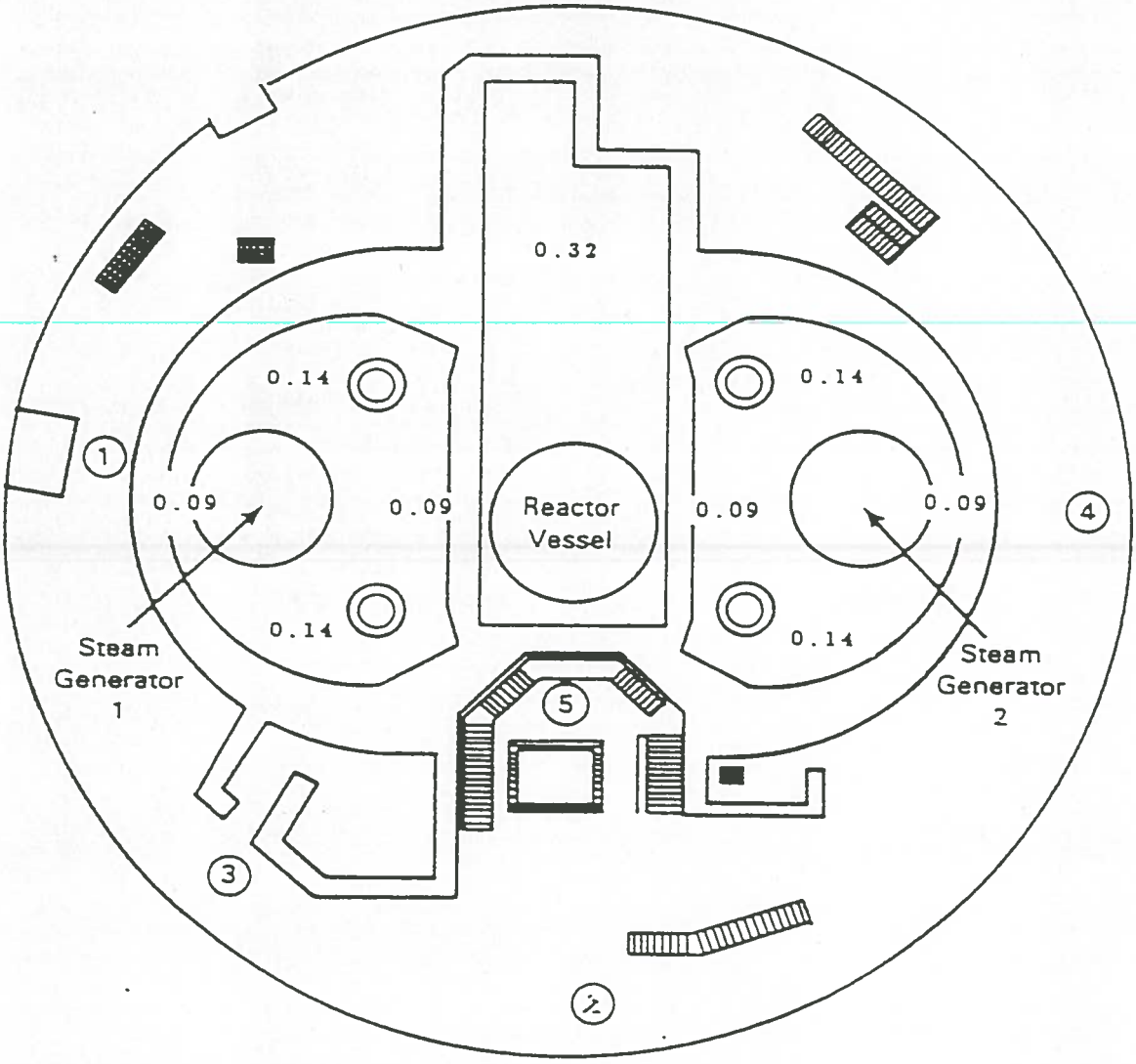

Figure 4-1. Location of Neutron Factors Inside the D-Rings

Table 4-7. Neutron Dose Equivalent Inside the D-Rings for Irradiation Period of 20.4 Days

Location	Avg.mR*	Gamma (mR)	mR* Neutron	NF	Dose (rem)
Refueling Cavity	7,795,000	440,640	7,354,360	0.32	2353.02
#2 S/G Hotleg	20,900,000	3,769,920	17,130,080	0.09	1541.75
#1 S/G Platform	1,575,000	4.504,320	-	0.09	-
#2 S/G Platform	6,720,000	4,504,320	2,215,680	0.09	199.27
#1B RCP Ladder	3,565,000	1,347,868	2,217,131	0.14	310.41
#2B RCP* Ladder	/	/	/	0.14	-
#1A RCP* Strainer	936,456	402,187	534,268	0.14	74.91
#1B RCP* Strainer	3,703,000	407,029	3,295,970	0.14	461.20
#1B RCP* Ladder	5.774,000	1,388,000	4,386,000	0.09	383.36
#2B RCP* Strainer	2,111,000	550,368	2,161,000	0.14	293.76

/ TLD Overranged

* Data Taken from First Survey (Es88)

The TLD at the #1 S/G platform neutron response was extremely low when compared to the response detected at the #2 S/G platform. As a result of this low response the neutron dose rate could not be determined since the average mR* minus the gamma dose calculated by QAD would result in no neutron dose. It is assumed that this particular TLD had been shielded by an unknown object during irradition. The #2B RCP ladder activation packet, which could not be retrieved from containment, had been left inside containment for approximately 150 days. As a result this TLD reached its limit of response (E1 and E2 approximately 60000 R*, E3 and E4 approximately 300 R*). This TLD gained no additional response after reaching its dose limit. All of the other locations surveyed produced dose rates ranging from 153 mrem/hr to 942 mrem/hr.

4.4 Total Dose Equivalent Rates Inside the D-Rings

The total dose equivalent rate for the radiation field present inside the D-rings is a combination of the neutron and gamma dose rates. With neutron dose rate results provided by TLDs and gamma dose rates calulated by QAD-CG, the dose rates for locations inside the D-rings were determined. Total dose equivalent rates for locations surveyed are in Table 4-8. Locations consisting of the #1 S/G platform, and #2B RCP ladder are not included in this table since neutron dose rates could not be determined. Because the #1 S/G hotleg packet was not retrieved from containment, it is assumed the dose rate determined for the #2 S/G hotleg can be applied to this location with minimal deviation. The same can also apply to other location dose rates such as applying the dose rate from the #1B RCP ladder in subsitution for the #2B RCP ladder.

Table 4-8 Total Dose Equivalent Rates Inside the D-Rings

Location	Neutron (rem/hr)	Gamma (rem/hr)	Total (rem/hr)
Refueling Cavity	4.806	0.900	5.706
#2 S/G Hotleg	3.149	7.719	10.87
#2 S/G Platform	0.407	9.200	9.607
#1B RCP Ladder	0.634	2.753	3.387
#1A RCP Strainer	0.153	0.797	0.950
#1B RCP Strainer	0.942	0.831	1.774
#2B RCP Strainer	0.600	1.124	1.724

.5 Conclusions and Recommendations

In all locations surveyed with the exception of the #1B RCP strainer, the ratio of neutron to gamma dose rates is dominated by gamma radiation inside the D-rings. This ratio demonstrates the effectiveness of the primary shield wall in degrading the neutron and gamma radiation originating from the reactor vessel. Although the secondary shield walls reduce the neutron and gamma radiation originating from the reactor vessel and reactor coolant primary loop, there is no way to avoid these high dose rates once the D-rings are entered.

Because the primary and secondary shield walls degrade (thermalize) the neutron spectra, TLD calibration factors presently applied by the algorithm in Figure 3-2 for neutron radiation may be too high. Because the NF applied in Figure 3-2 for neutrons is 0.70, an individual exposed to a more thermalized spectra could have a reported dose double the actual dose. The neutron factor of 0.70 is generated from a D_2O moderated ^{252}Cf source which is a harder spectrum than that found at Waterford. The neutron spectrum produced by the HPRR was demonstrated to have a spectrum similar to that found in nuclear power plants as demonstrated by the comparison to ANO-2. Therefore the NF generated by the HPRR of 0.32 appears to be more appropriate for the hardest neutron spectra inside containment at Waterford and other nuclear power plants. In light of this theory, it is also suggested that TLD calibration factors used at nuclear power plants should be those generated by the concrete, steel, and lucite shielded HPRR.

Even though the dose rates inside the D-rings are quite high in most locations surveyed, it appears that entry for short stay times is

feasible. Since the dose rates for the RCP ladders are high, and streaming paths from piping penetrations would be encountered, entry from the bottom of the D-rings is not recommended. If the entry is made from the top of the D-rings, streaming paths would not be crossed. This entry pathway would allow access to the RCP strainers or other components inside the D-rings with the minimum dose. Access to all other locations inside the D-rings (i.e. locations near the S/G hotleg and S/G plenum) is not recommended at full power.

The use of QAD-CG proved to be a very valuable tool for determining the dose rates inside the D-rings. QAD results provided the gamma dose rates needed to evaluate and obtain the neutron response on the TLDs. QAD allowed the activation samples to reach saturation activity with less concern about overranging the gamma dosimetry of the TLDs. QAD possesses the ability to place as many detectors in a particular model as needed for a single run which helped cut down on the modeling time. Lastly, the product of using QAD resulted in a model that can be used in the future to calculate gamma dose rates inside the D-rings by placing detectors at the desired locations with no further modeling needed. In spite of these advantages QAD does have drawbacks. QAD is only as good as the mathmatical model representing the real situation. Accurate description of the source is also especially important to derive an acceptable answer.

It is recommended that further studies be conducted inside the D-rings. Activation packets should be used to further characterize the true neutron spectrum. These packets should include activation targets that cover a larger portion of the neutron spectrum. It is also

recommended those locations at the RCP ladders and other areas above the RCP strainers be resurveyed to confirm that no other streaming paths are encountered before an entry path is assigned.

Use of the NF of 0.32 for the most conservative estimate of neutron dose equivalent for all locations inside containment is recommended since this neutron factor is established in the hardest spectra (refueling cavity). Lastly it recommended that the NFs estimated inside the D-rings be reevaluated using a TEPC and Panasonic 802 TLDs at 10 or 20 percent of full power and extrapolate the results to 100% power. Generating NFs from these results will confirm or establish new NFs for inside the D-rings.

REFERENCES

(ANSI83) Personnel Dosimetry Performance - Criteria for Testing, American National Standards Institute, N13.11, 1983

(ASTM) The Standard Method for Determining Thermal Neutron Reaction and Fluence Rates by Radioactivation Techniques, E262-86

(Au68) J.A. Auxier, W.S. Snyder, and T.D. Jones; "Neutron Interactions and Penetration in Tissue", Radiation Dosimetry, Vol. 1,1968

(Be64) K.H. Beckurts and K. Wirtz; Neutron Physics, Springer-Verlag, 1964

(Ca77) V.R. Cain; A Users Manual for QAD-CG, Bechtel Power Corporation 1977

(Ch79) A.B. Chilton and S. Chen; "Calculation of Fast Neutron Depth Dose in the ICRU Standard Tissue Phantom and the Derivation of Neutron Fluence to Dose Index Conversion Factors", Radiation Research 78, 1979

(Cl87) S. Clark; Waterford 3 Containment Neutron Dose Rate Profile, Waterford Document W31051HP, 1987

(De72) D. DeSoete, R. Gijbels, and J. Hoste; Neutron Activation Analysis, Wiley and Sons, London, 1972

(Eb88) Eberline PNR-4, RO2; Eberline Technical Users Manual, 1988

(En81) G. Endres, J. Aldrich, L. Brackenbush, L. Faust, R. Griffith, D. Hankins; Neutron Dosimetry at Commercial Nuclear Power Plants, NUREG/CR-1769, 1981

(Es88) G. Espenan; Measurement of the Dose Equivalent Rates Inside the D-Rings at Power, Waterford Document W390754SA, 1988

(FSAR88) Waterford 3 Final Safety Analysis Report, Revision 2, 1988

(Ha78) D. Hankins and R. Griffith; A Survey of Neutrons Inside the Containment of a Pressurized Water Reactor, UCRL-81346, 1978

(ICRP71) Data for Protection Against Ionizing Radiation From External Sources, International Commission on Radiation Protection Report No. 21, 1971

(Ly64) W. Lyon; A Guide to Neutron Activation Analysis, D. Van Nostrand Co., Princeton, N.J., 1964

(Ma67) R. Malenfant; QAD a Series of Point Kernel General Purpose Shielding Programs, LA-3572, 1967

(Mi87) MICROSHIELD; Grove Engineering Inc., Rockville, MD, 1987

(NCRP38) National Council on Radiation Protection Report No. 38, 1971

(NSSS82) Nuclear Steam Supply System Description, Combustion Engineering, 1982

(Pl83) P. Plato and J. Miklos; "Response of the Panasonic UD-802 Dosimeter to Neutrons of Various Energies", University of Michigan School of Public Health, 1983

(Si87) C. Sims and G. Ragan; Health Physics Research Reactor Reference Dosimetry, ORNL-6240,1987

(So85) K. Soldat, D. Haggard, J. Tanner, and P. Tomerassen; Neutron Dose and Energy Spectral Measurements Inside Reactor Containment at Waterford 3 SES, Batelle Northwest, 1985

St70) E. Straker, P. Stevens, D. Irving, and V. Cain; The Morse Code-A Multigroup Neutron and Gamma Ray Monte Carlo Transport Code, ORNL-4584, 1970

Ts85) N. Tsoulfandis; Neutron Energy Spectra in the Core and Cavity of the ANO-2 PWR, EPRI, NP4238, 1985

APPENDIX A

Input for the QAD-CG Program Describing the Reactor Vessel Source

```
    WATERFORD 3  CONTAINMENT: REACTOR AS THE SOURCE
     23  50   24  12    8   5   13   6    0   2    1   0    0    0    0   0
   2.147+6
0          10.61     20.32     30.48     40.64     50.8      60.96     71.12
81.28      91.44     101.6     111.76    121.92    132.08    142.24    152.4
162.56     172.72    193.04    203.2     213.36    223.52    233.68    243.84
0          28.04     56.08     84.12     112.16    140.2     168.24    196.28
224.32     252.36    280.4     308.44    336.48    364.52    392.56    420.60
448.64     476.68    504.72    532.76    560.8     588.84    616.88    644.92
672.96     701.0     729.04    757.08    785.12    813.16    841.2     869.24
897.28     925.32    953.36    981.4     1009.44   1037.48   1065.52   1093.56
1121.6     1149.64   1177.68   1205.72   1233.76   1261.8    1289.84   1317.88
1345.92    1373.96   1402.08
0          .262      .5236     .785      1.0472    1.31      1.5708    1.83
2.094      2.36      2.618     2.88      3.1416    3.4       3.665     3.93
4.188      4.46      4.712     4.97      5.26      5.49      5.76      6.62
6.283
                                1    0                1.0   WATERFORD 3 CONTAINMENT
 RPP      -5000.0    5000.0    -5000.0   5000.0    -1000.0   5000.0
 RCC      0                    0                                       1402.08
          243.84
 RCC      0                    0                                       1097.0
          335.28
 RCC      0.0        335.28    914.4     0.0       198.12    0.0
          121.92
 RCC      0.0        121.92    914.4     0.0       518.16    0.0
          49.53
 RCC      0.0        121.92    914.4     0.0       518.16    0.0
          53.34
 RPP      -960.0     960.0     -563.88   563.88    0.0       1097.0
 RPP      -975.4     975.4     381.0     548.64    1097.28   2590.80
 RPP      -975.4     975.4     1371.6    1492.52   0.0       2590.80
 RCC      0.0        0.0       1402.08   0.0       0.0       457.20
          243.84
 RCC      -213.36    121.92    914.4     -152.4    83.82     0.0
          121.92
 RCC      -320.04    160.02    914.4     -220.98   320.04    0.0
          121.92
 RCC      -213.36    121.92    914.4     -152.4    83.82     0.0
          42.67
 RCC      -335.28    198.12    914.4     -198.12   320.04    0.0
          42.67
 RCC      -213.36    121.92    914.4     -152.4    83.82     0.0
          45.72
```

```
RCC     -335.28   198.12    914.4     -198.12   320.04    0.0
        45.72
RCC     213.36    121.92    914.4     182.88    106.68    0.0
        121.92
RCC     335.28    121.92    914.4     0.0       426.72    0.0
        121.92
RCC     213.36    121.92    914.4     144.78    88.39     0.0
        42.67
RCC     335.28    152.4     914.4     0.0       487.68    0.0
        42.67
RCC     213.36    121.92    914.4     144.78    88.39     0.0
        45.72
RCC     335.28    152.4     914.4     0.0       487.68    0.0
        45.72
RCC     -457.2    746.76    850.0     0.0       0.0       609.6
        100.4
RCC     457.2     746.76    850.0     0.0       0.0       609.6
        100.4
RCC     0.0       1249.68   850.0     0.0       0.0       944.88
        220.98
TRC     0.0       1249.68   1794.88   0.0       0.0       213.36
        220.98    335.38
RCC     0.0       1249.68   2008.24   0.0       0.0       976.36
        335.28
RPP     -854.48   -975.4    548.64    1371.6    0.0       2590.0
RPP     854.48    975.4     548.64    1371.6    0.0       2590.0
END
1           2
2           3     -2
3           4     -5      -6
4           5
5           6     -5
6           7     -2      -3      -4      -5      -6      -11     -12
          -13     -14     -15     -16     -17     -18     -19     -20
          -21     -22
7           8
8           9
9          10
10         11     -13     -15
11         12     -14     -16
12         13
13         14
14         15     -13
```

```
15              16    -14
16      OR  +11   +12   -13   -14   -15   -16
17      OR  +13   +14
18      OR  +15   +16   -13   -14
19          17    -19   -21
20          18    -20   -22
21          19
22          20
23          21    -19
24          22    -20
25      OR  +17   +18   -19   -20   -21   -22
26      OR  +21   +22   -19   -20
27      OR  +19   +20
28          23    -14   -16
29          24    -20   -22
30          25
31          26
32          27
33          28
34          29
35           1    -2    -3    -4    -5    -6    -7    -8
            -9   -10   -11   -12   -13   -14   -15   -16
           -17   -18   -19   -20   -21   -22   -23   -24
           -25   -26   -27   -28   -29
END
  1   1   1   1   1   1   1   1   1   1   1   1   1   1
  1   1   1   1   1   1   1   1   1   1   1   1   1   1
  1   1   1   1   1   1   1
  1   1   1   3   5   2   2   2   6   1   1   3   3   5
  5   1   3   5   1   1   3   3   5   5   1   5   3   8
  8   8   7   7   2   2   1
  6   1   8  13  14  20  26  92  48  13  24  28  41
0.0      .001     0.0      0.0      0.0      0.0      0.0      0.0
0.0      0.0      0.0      0.0
.00916   .899     .12      .617     .1006    .0555    0.0      0.0
0.0      0.0      0.0      0.0
.1111    .8889    0.0      0.0      0.0      0.0      0.0      0.0
0.0      0.0      0.0      0.0
0.0      0.0      0.0      0.0      0.0      0.0      18.90    0.0
0.0      0.0      0.0      0.0
0.0      0.0      0.0      0.0      0.0      7.86     0.0      0.0
```

0.0	0.0	0.0	0.0				
0.0	0.0	0.0	0.0	0.0	0.0	0.0	8.65
0.0	0.0	0.0	0.0				
0.0	0.0	0.0	0.0	0.0	0.0563	0.0	0.0
0.0	1.15	6.54	0.1966				
0.00275	0.2666	0.0	0.0	0.0	0.4151	0.0	0.0
0.0	0.805	4.57	0.1376				

0.15	.50	.75	1.00	1.5	2.5	3.5	4.5
5.5	6.5	7.5	8.5	9.5			
3.790+9	1.960+9	8.231+8	1.143+9	2.510+9	1.400+9	9.450+8	7.430+8
5.994+8	5.480+8	4.976+8	2.626+8	3.050+7			
.0024	1.293-3	1.818-3	1.283-3	1.563-3	1.408-3	1.235-3	1.136-3
1.099-3	1.020-3	1.000-3	0.909-3	0.833-3			
1.0	1.0	1.0	1.0	1.0	1.0	1.0	1.0
1.0	1.0	1.0	1.0	1.0			

.1-10.0						
.1-.25	.25-.6	.6-0.8	0.8-1.25	1.25-1.75	1.75-3.00	
3.0-4.0	4.0-5.0	5.0-6.0	6.0-7.0	7.0-8.0	8.0-9.0	
9.0-10.0						

MEV/CM*2-SEC		MREM/HR		N/A
-411.48	975.36	883.92	1	
0.0	975.36	670.56	1	
0.0	975.36	1280.16	1	
426.72	975.36	929.64	1	
-259.10	396.24	112.52	1	
			-1	

APPENDIX B

Input for the QAD-CG Program Describing the Steam Generator Hotleg Plenum Source

```
   WATERFORD 3  CONTAINMENT: STEAM GENERATOR AS THE SOURCE
    23  23   24  12    8   5    6   6    0   2    1   0    0   0    0   0
       1.0
0          9.608     19.216    28.823    38.431    48.039    57.647    67.255
76.863     86.47     96.07     105.68    115.29    124.90    134.50    144.12
153.72     163.33    172.94    182.55    192.15    201.76    211.37    220.98
0          6.604     13.208    19.812    26.416    33.020    39.624    46.228
52.832     59.436    66.040    72.644    79.248    85.852    92.456    99.060
105.664    112.268   118.872   125.476   132.080   138.864   145.288   151.892
0          .262      .5236     .785      1.0472    1.31      1.5708    1.83
2.094      2.36      2.618     2.88      3.1416    3.4       3.665      3.93
4.188      4.46      4.712     4.97      5.26      5.49      5.76      6.62
6.283
                        1    0              1.0   WATERFORD 3 CONTAINMENT
  RPP      -5000.0    5000.0    -5000.0    5000.0    -1000.0    5000.0
  RCC      0.0        0.0       0.0        0.0       0.0        59.8
           220.98
  RCC      0.0        0.0       59.8       0.0       0.0        885.08
           220.98
  TRC      0.0        0.0       944.88     0.0       0.0        213.36
           220.98     335.38
  RCC      0.0        0.0       1158.24    0.0       0.0        976.36
           335.28
  RPP      -975.36    975.36    -601.98    -434.34   -850.0     1740.80
  RPP      -975.36    -853.44   -434.34    396.24    -850.0     1740.8
  RPP      -975.36    975.36    396.24     518.16    -850.0     1740.8
  RPP      853.44     975.36    -434.34    396.24    -850.0     1740.8
  RCC      -457.2     -243.84   0.0        0.0       0.0        609.6
           100.4
  RCC      457.2      -243.84   0.0        0.0       0.0        609.6
           100.4
  END
  1              2
  2              3
  3              4
  4              5
  5              6
  6              7
  7              8
  8              9
  9             10
  10            11
  11             1     -2     -3     -4     -5     -6     -7     -8
                -9    -11
  END
    1    1    1    1    1    1    1    1    1    1    1
    3    8    3    3    2    2    2    2    7    7    1
    1    1    8   13   14   20   26   92   48   13   24   28   41
```

```
0.0         .001        0.0         0.0         0.0         0.0         0.0         0.0
0.0         0.0         0.0         0.0
.00916      .899        .12         .617        .1006       .0555       0.0         0.0
0.0         0.0         0.0         0.0
.1111       .8889       0.0         0.0         0.0         0.0         0.0         0.0
0.0         0.0         0.0         0.0
0.0         0.0         0.0         0.0         0.0         0.0         18.90       0.0
0.0         0.0         0.0         0.0
0.0         0.0         0.0         0.0         0.0         7.86        0.0         0.0
0.0         0.0         0.0         0.0
0.0         0.0         0.0         0.0         0.0         0.0         0.0         8.65
0.0         0.0         0.0         0.0
0.0         0.0         0.0         0.0         0.0         0.0563      0.0         0.0
0.0         1.15        6.54        0.1966
0.02222     0.1778      0.0         0.0         0.0         0.3321      0.0         0.0
0.0         0.8912      5.69        0.0
     0.044      0.284      0.679      1.215      2.303      6.129
  1.77+12  6.105+11   1.658+12   1.915+12   6.121+11   2.139+14
   3.45-3     1.85-3     1.96-3     1.78-3     1.58-3     1.07-3
   1.0        1.0        1.0        1.0        1.0        1.0
.01-6.5
.01-.10       .10-.5        .5-1.0        1.0-2.0       2.0-2.5       6.0-6.5
MEV/CM*2-SEC                MREM/HR                     N/A
-411.48     121.92     -91.44          1
0.0         60.96      335.28          1
0.0         60.96      304.8           1
246.72      121.92     60.96           1
-259.10     -548.64    91.44           1
                                       -1
```

APPENDIX C

Nuclide Energy Groups for Hotleg Plenum

Nuclides in the Average Energy Range of 0.01-0.10 (MeV) in the Steam Generator Hotleg Plenum

Nuclide	Curies	MeV/sec
^{83m}Kr	0.2103	4.096E+6
^{127m}Te	0.0042	4.698E+4
^{133}Xe	189.50	2.102E+11
Total:	189.72	2.102E+11

Average Gamma Energy for Group: 0.044 (MeV)

Nuclides in the Average Energy Range of 0.10-0.50 (MeV) in the Steam Generator Hotleg Plenum

Nuclide	Curies	MeV/sec
^{135}Xe	3.5170	2.926E+10
^{133m}Xe	2.2540	1.944E+10
^{131m}Xe	1.2160	7.371E+9
^{85m}Kr	1.1030	4.646E+9
^{132}Te	0.3685	2.738E+9
^{131}I	4.0170	4.388E+10
^{127}Te	0.0101	1.540E+6
^{239}Np	0.0168	1.260E+7
^{99m}Tc	4.3110	1.994E+11
^{51}Cr	0.0286	3.319E+7
Totals:	16.842	3.067E+11

Average Gamma Energy for Group: 0.212 (MeV)

Nuclides in the Average Energy Range of 0.50-1.00 (MeV) in the Steam Generator Hotleg Plenum

Nuclide	Curies	MeV/sec
^{85}Kr	2.2950	4.347E+10
^{137m}Ba	0.1601	3.547E+9
^{136}Cs	0.1799	5.440E+9
^{134}Cs	0.3542	7.735E+9
^{134}I	0.4826	1.431E+10
^{133}I	4.9050	6.866E+10
^{132}I	1.0620	4.926E+9
^{131m}Te	0.0332	7.223E+7
^{130}I	0.0256	5.041E+8
^{89}Sr	0.0053	1.653E+4
^{83}Br	0.0511	9.815E+8
^{58}Co	0.2417	7.207E+9
^{54}Mn	0.0047	1.451E+8
Totals:	9.6160	1.516E+11

Average Gamma Energy: 0.679 (MeV)

Nuclides in the Average Energy Range of 1.0-2.0 (MeV) in the Steam Generator Hotleg Plenum

Nuclide	Curies	MeV/sec
^{135}I	2.1790	2.906E+10
^{138}Xe	0.403	4.041E+9
^{91}Y	0.0302	4.038E+6
^{89}Kr	0.0500	1.084E+6
^{88}Kr	2.0040	6.137E+10
^{86}Rb	0.0012	4.618E+6
^{60}Co	0.0304	2.807E+9
^{59}Fe	0.0151	3.138E+8
Totals:	4.7130	9.760E+10

Average Gamma Energy for Group: 1.215 (MeV)

Nuclides in the Average Energy Range of $\geq$ 2.00 (MeV) in the Steam Generator Hotleg Plenum

Nuclide	Curies	MeV/sec
^{16}N	242.67	2.531E+12

Average Gamma Energy for Group: 6.622 (MeV)

APPENDIX D

Input for the QAD-CG Program Describing the Generator Tubing Source

```
   WATERFORD 3  CONTAINMENT: STEAM GENERATOR AS THE SOURCE
    23  23   24  12    8   5    6   6    0   2    1   0    0   0    0   0
       1.0
0          9.61     19.21     28.82     38.43     48.04     57.65     67.25
76.86     86.47     96.07     105.68    115.29    124.90    134.50    144.12
153.72    163.33    172.94    182.55    192.15    201.76    211.37    220.98
0         41.082    82.163    123.24    164.327   205.409   246.49    287.572
328.865   369.736   410.817   451.899   492.981   534.063   575.144   616.226
657.308   698.390   739.471   780.553   821.653   862.717   903.798   944.880
0         .262      .5236     .785      1.0472    1.31      1.5708    1.83
2.094     2.36      2.618     2.88      3.1416    3.4       3.665      3.93
4.188     4.46      4.712     4.97      5.26      5.49      5.76      6.62
6.283
                      1    0              1.0   WATERFORD 3 CONTAINMENT
  RPP      -5000.0    5000.0    -5000.0   5000.0    -1000.0   5000.0
  RCC      0.0        0.0       0.0       0.0       0.0       944.88
           220.98
  TRC      0.0        0.0       944.88    0.0       0.0       213.36
           220.98     335.38
  RCC      0.0        0.0       1158.24   0.0       0.0       976.36
           335.28
  RPP      -975.36    975.36    -601.98   -434.34   -850.0    1740.80
  RPP      -975.36    -853.44   -434.34   396.24    -850.0    1740.8
  RPP      -975.36    975.36    396.24    518.16    -850.0    1740.8
  RPP      853.44     975.36    -434.34   396.24    -850.0    1740.8
  RCC      -457.2     -243.84   0.0       0.0       0.0       609.6
           100.4
  RCC      457.2      -243.84   0.0       0.0       0.0       609.6
           100.4
  END
  1              2
  2              3
  3              4
  4              5
  5              6
  6              7
  7              8
  8              9
  9             10
  10             1     -2     -3     -4     -5     -6     -7     -8
                -9    -10
  END
    1    1    1    1    1    1    1    1    1    1
    8    3    3    2    2    2    2    7    7    1
    3    1    8   13   14   20   26   92   48   13   24   28   41
```

0.0	.001	0.0	0.0	0.0	0.0	0.0	0.0
0.0	0.0	0.0	0.0				
.00916	.899	.12	.617	.1006	.0555	0.0	0.0
0.0	0.0	0.0	0.0				
.1111	.8889	0.0	0.0	0.0	0.0	0.0	0.0
0.0	0.0	0.0	0.0				
0.0	0.0	0.0	0.0	0.0	0.0	18.90	0.0
0.0	0.0	0.0	0.0				
0.0	0.0	0.0	0.0	0.0	7.86	0.0	0.0
0.0	0.0	0.0	0.0				
0.0	0.0	0.0	0.0	0.0	0.0	0.0	8.65
0.0	0.0	0.0	0.0				
0.0	1.15	6.54	0.1966	0.0	0.0563	0.0	0.0
0.02222	0.1778	0.0	0.0	0.0	0.3321	0.0	0.0
0.0	0.8912	5.69	0.0				

0.044	0.284	0.679	1.215	2.303	6.129	
2.10+11	1.134+11	1.516+11	2.346+11	6.822+10	5.503+13	
3.45-3	1.85-3	1.96-3	1.78-3	1.58-3	1.11-3	
1.0	1.0	1.0	1.0	1.0	1.0	

.01-6.5						
.01-.10	.10-.5	.5-1.0	1.0-2.0	2.0-2.5	6.0-6.5	
MEV/CM*2-SEC		MREM/HR		N/A		
-411.48	121.92	-91.44	1			
0.0	60.96	335.28	1			
0.0	60.96	304.8	1			
246.72	121.92	60.96	1			
-259.10	-548.64	91.44	1			
			-1			

APPENDIX E

Nuclide Energy Groups for Steam Generator Tubing

Nuclides in the Average Energy Range of 0.01-0.10 (MeV) in the Steam Generator Tubing

Nuclide	Curies	MeV/sec
^{83m}Kr	1.7780	3.460E+7
^{127m}Te	0.0358	3.969E+5
^{133}Xe	1602.6	1.770E+12
Total:	1604.5	1.770E+12

Average Gamma Energy for Group: 0.044 (MeV)

Nuclides in the Average Energy Range of 0.10-0.50 (MeV) in the Steam Generator Tubing

Nuclide	Curies	MeV/sec
^{135}Xe	29.740	2.474E+11
^{133m}Xe	19.050	1.644E+11
^{131m}Xe	10.280	6.234E+10
^{85m}Kr	34.682	1.459E+11
^{132}Te	3.1155	2.320E+10
^{131}I	33.969	3.711E+11
^{127}Te	0.0851	1.303E+7
^{239}Np	0.1420	1.066E+8
^{99m}Tc	36.448	1.680E+12
^{51}Cr	0.2419	2.807E+8
Totals:	167.75	2.694E+12

Average Gamma Energy: 0.212 (MeV)

Nuclides in the Average Energy Range of 0.50-1.0 (MeV) in the Steam Generator Tubing

Nuclide	Curies	MeV/sec
^{85}Kr	19.405	3.675E+11
^{137m}Ba	1.3530	2.991E+10
^{136}Cs	1.5209	4.603E+10
^{134}Cs	2.9950	6.540E+10
^{134}I	4.0809	1.221E+11
^{133}I	41.473	5.810E+11
^{132}I	89.780	4.165E+11
^{131m}Te	0.2807	6.120E+8
^{130}I	0.2171	4.260E+9
^{89}Sr	0.0447	1.398E+5
^{83}Br	0.4322	8.262E+9
^{58}Co	2.0440	6.095E+10
^{54}Mn	0.0347	1.084E+9
Totals:	163.194	1.689E+12

Average Gamma Energy: 0.679 (MeV/dis)

Nuclides in the Average Energy Range of 1.0-2.0 (MeV) in the Steam Generator Tubing

Nuclide	Curies	MeV/sec
^{135}I	18.425	2.457E+11
^{138}Xe	3.7232	3.416E+10
^{91}Y	0.2553	3.410E+7
^{89}Kr	0.4231	9.169E+7
^{88}Kr	16.945	5.187E+11
^{86}Rb	0.0101	3.522E+7
^{60}Co	0.2566	5.920E+10
^{59}Fe	0.1273	3.428E+9
Totals:	40.165	8.578E+11

Average Gamma Energy for Group: 1.215 (MeV)

Nuclides in the Average Energy Range of $\geq$ 2.00 (MeV) in the Steam Generator Tubing

Nuclide	Curies	MeV/sec
^{16}N	2049.9	2.138E+13

Average Gamma Energy for Group: 6.622 (MeV)

VITA

Duane Foster McLane, was born on November 29, 1963, in San Diego California, to David J. McLane and Juanita Y. McLane. He attended high school in Hahnville, Lousiana. After graduation in the spring of 1982 he enrolled at Louisiana State Universtiy. In May, 1987, he graduated with a Bacholors Degree in Engineering Technology. In the fall of 1987 he entered graduate school at Louisiana State University under the department of Nuclear Science. He is presently a candidate for a M.S. degree in Nuclear Science, Radiation Protection Option.

MASTER'S EXAMINATION AND THESIS REPORT

Candidate: Duane Foster McLane

Major Field: Nuclear Science

Title of Thesis: A Determination of the Neutron and Gamma Dose Rates Inside the D-Rings at the Waterford 3 Pressurized Water Reactor

Approved:

John Courtney
Major Professor and Chairman

F. Glenn Kemby
Dean of the Graduate School

EXAMINING COMMITTEE:

M. L. Williams

L. M. Scott

A. D. Sperson

Date of Examination:

June 9, 1989